Dissertation

VTT PUBLICATIONS 758

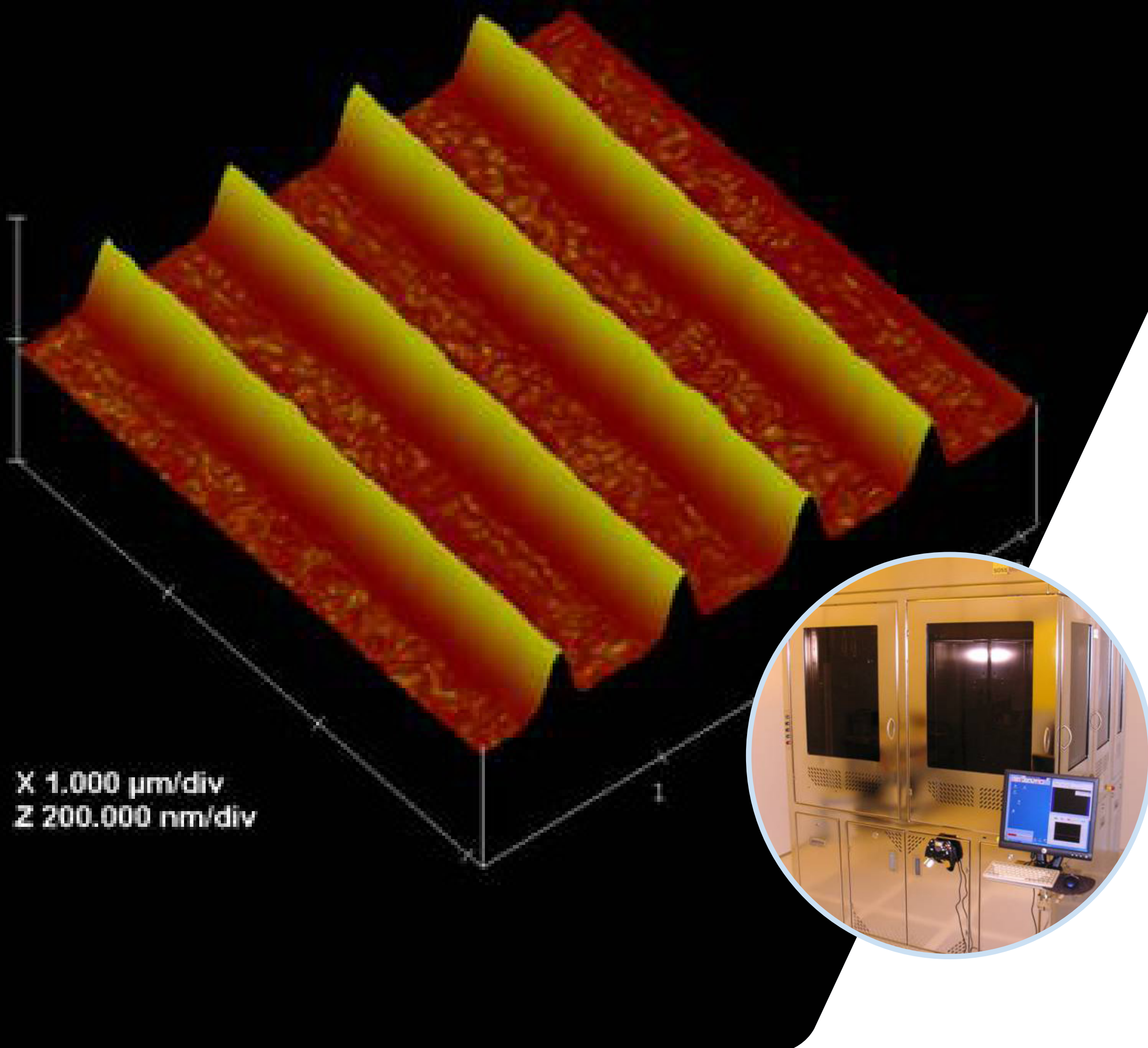

Tomi Haatainen

Stamp fabrication by step and stamp nanoimprinting

VTT

VTT PUBLICATIONS 758

Stamp fabrication by step and stamp nanoimprinting

Tomi Haatainen

Dissertation for the degree of Doctor of Philosophy to be presented with due permission of School of Electrical Engineering for public examination and debate in Large Seminar Hall of Micronova at Aalto University, School of Electrical Engineering (Espoo, Finland) on the 1st of April 2011 at 12 noon.

ISBN 978-951-38-7726-2 (softback ed.)
ISSN 1235-0621 (softback ed.)

ISBN 978-951-38-7727-9 (URL: http://www.vtt.fi/publications/index.jsp)
ISSN 1455-0849 (URL: http://www.vtt.fi/publications/index.jsp)

Copyright © VTT 2011

JULKAISIJA – UTGIVARE – PUBLISHER

VTT, Vuorimiehentie 5, PL 1000, 02044 VTT
puh. vaihde 020 722 111, faksi 020 722 4374

VTT, Bergsmansvägen 5, PB 1000, 02044 VTT
tel. växel 020 722 111, fax 020 722 4374

VTT Technical Research Centre of Finland, Vuorimiehentie 5, P.O. Box 1000, FI-02044 VTT, Finland
phone internat. +358 20 722 111, fax + 358 20 722 4374

Edita Prima Oy, Helsinki 2011

Tomi Haatainen. Stamp fabrication by step and stamp nanoimprinting [Painomuottien valmistus sekventiaalista nanokuviointimenetelmää käyttäen]. 2011. VTT Publications 758. 70 p. + app. 59 p.

Keywords nanoimprinting, hot embossing, stamp replication

Abstract

The nanoimprinting is a potential method for submicron scale patterning for various applications, for example, electric, photonic and optical devices. The patterns are created by mechanical deformation of imprint resist using a patterned imprinting mold called also a stamp. The bottle-neck for imprint lithography is availability of the stamps with nanometer-scale features, which are typically fabricated by electron beam lithography. Therefore, patterning of a large stamp is time consuming and expensive. Nanoimprint lithography can offer a low cost and a high through-put method to replicate these imprinting molds.

In this work, stamp replication process was developed and demonstrated for three different types of imprint molds. Replication relies on sequential patterning method called step and stamp nanoimprint lithography (SSIL). In this method a small master mold is used to pattern large areas sequentially. The fabricated stamps are hard stamps for thermal imprinting, bendable metal stamps for roll embossing and transparent stamps for UV-imprinting.

Silicon is a material often used for fabrication of hard stamps for thermal imprinting. Fabrication process of silicon stamps was demonstrated using both the imprinted resist and lift-off process for pattern transfer into silicon.

Bendable metal stamp for roll-to-roll application was fabricated using sequential imprinting to fabricate a polymer mold. The polymer mold was used for fabrication of a nickel copy in subsequent electroplating process. Thus fabricated metal stamp was used in a roll-to-roll imprinting process to transfer the patterns onto a CA film successfully.

Polymer stamp for UV-imprinting was fabricated by patterning fluorinated polymer templates using sequential imprinting and a silicon stamp. The imprinted polymer stamp was used succesfully for UV-NIL.

In the stamp fabrication process the features of the silicon stamp were replicated with good fidelity, retaining the original dimensions in all of three stamp types. The results shows, that the sequential imprinting is as a potential stamp replication method for various applications.

Tomi Haatainen. Stamp fabrication by step and stamp nanoimprinting [Painomuottien valmistus sekventiaalista nanokuviointimenetelmää käyttäen]. 2011. VTT Publications 758. 70 s. + liitt. 59 s.

Keywords nanoimprinting, hot embossing, stamp replication

Tiivistelmä

Nanoimprint-litografia on noussut varteenotettavaksi ehdokkaaksi nanorakenteiden kuvioinnissa. Tähän asti käytetty optinen litografia on toistaiseksi kyennyt vastaamaan haasteeseen viivanleveyden pienentyessä. Menetelmän kehittäminen johtaa yhä kalliimpiin ja teknisesti mutkikkaampiin ratkaisuihin. Pienempiin viivanleveyksiin on mahdollista käyttää esim. elektronisuihkulitografiaa, mutta menetelmän haittapuolena on massatuotannon esteeksi nouseva hitaus, mikä nostaa kustannuksia.

Nanoimprint-litografian pullonkaulana on ollut painomuottien eli leimasinten valmistus, joka tapahtuu elektronisuihkulitografialla. Pinta-alaltaan suurien muottien valmistus on hidasta ja tulee erittäin kalliiksi. Vaihtoehtoisesti voidaan valmistaa pieni muotti, jota toistamalla voidaan kuvioida laajoja alueita. Tällä menetelmällä voidaan tehdä suuri määrä kopioita alkuperäisestä muotista tai valmistaa suuri kokonaisuus yhdistelemällä erityyppisiä pieniä muotteja.

Tämän väitöskirjatyön aiheena on painomuottien valmistaminen step and stamp nanoimprint-litografiamenetelmällä. Työn kokeellinen osa käsittää prosessiparametrien optimoinnin laajojen alueiden kuviointiin sekä muottien valmistuksen ja kopioinnin termoplastiseen polymeeriin. Kuviointi tehtiin käyttämällä piistä valmistettua muottia eli leimasinta. Leimasimet valmistettiin pääosin piistä käyttämällä UV- tai elektronisuihkulitografiaa sekä kuivaetsausta. Menetelmää sovellettiin piipainomuottien kopiointiin, valmistettiin nikkelinen taipuisa painomuotti rullapainomenetelmää varten sekä läpinäkyvä polymeeripainomuotti UV-imprint-litografiaa varten.

Preface

This work has been carried out between 1999 and 2009 at VTT Technical Research Centre of Finland in Espoo. The work was initiated in the Materials and Packaking Group at Microelectronics Centre. The name and the organization of the author´s research group have changed few times during these years. Presently, the author is a member of the Nanoelectronics team. Most of the research work was performed in EU funded projects including NANOTECH (project No. 28785), CHANIL (IST-1999-13415), NAPA (NMP-4-CT-2003-500120) and NAPANIL (NMP-2007-3.5-1).

I wish to thank Prof. Jouni Ahopelto for his guidance during this work. The supervisor Prof. Pekka Kuivalainen is acknowledged for his valuable comments on the manuscript and advices with practical issues related to doctoral dissertation. I would like to give special thanks to my colleague Dr. Tapio Mäkelä for his comments on the manuscript and many fruitful discussions. I am also grateful to Päivi Majander who took part into the research work and publishing of the results. Also Dr. Mika Prunnila and Sanna Arpiainen are gratefully thanked. I would also thank Jorma Salmi and Jaakko Salonen for their patience and guidance when I was introduced to the use of the flip chip bonder. I would also like to express my gratitude to the Prof. Jouni Heleskivi, Ilkka Suni and Prof. Jorma Kivilahti for the support helping to conduct this work. The work would have been impossible to conduct without priceless guidance and assistance of clean room technicians Kristiina Rutanen, Meeri Partanen, Merja Markkanen, Liisa Valkonen and Mervi Hämäläinen. I would also like to thank all the other present and former colleagues at VTT for offering numerous contributions and inspiration to my work.

I want to thank my parents for supporting my studies and also my brother Kai who encouraged me to continue the studies in the academic world. I thank all my relatives and friends for support and helping to loosen up sometimes. Finally, I wish to thank Maritta for her patience and for standing besides me all these years.

List of publications

I Haatainen, T., Ahopelto, J., Gruetzner, G., Fink, M. and Pfeiffer, K. Step & stamp imprint lithography using commercial flip chip bonder. Proc. SPIE. 3997 (2000), pp. 874–880.

II Haatainen, T. and Ahopelto, J. Pattern Transfer using Step & Stamp Imprint Lithography. Phys. Scri. 67(4) (2003), pp. 357–360.

III Haatainen, T., Majander, P., Riekkinen, T. and Ahopelto, J. Nickel stamp fabrication using step & stamp imprint lithography. Microelectron. Eng. 83 (2006), pp. 948–950.

IV Mäkelä, T., Haatainen, T., Majander, P., Ahopelto, J. and Lambertini, V. Continuous Double-Sided Roll-to-Roll Imprinting of Polymer Film. Jpn. J. Appl. Phys. 47(6) (2008), pp. 5142–5144.

V Haatainen, T., Majander, P., Mäkelä, T., Ahopelto, J. and Kawaguchi, Y. Imprinted 50 nm Features Fabricated by Step and Stamp UV Imprinting. Jpn. J. Appl. Phys. 47(6) (2008), pp. 5164–5166.

VI Haatainen, T., Mäkelä, T., Ahopelto, J., and Kawaguchi,Y. Imprinted polymer stamps for UV-NIL. Microelectron. Eng. 86(11) (2009), pp. 2293–2296.

VII Courgon, G., Chaix, N., Schift, H., Tormen, M., Landis, S., Sotomayor Torres, C., Kristensen, A., Pedersen, R. H., Christiansen, M. B., Fernandez-Cuesta, I., Mendels, D., Montelius, L. and Haatainen, T. Benchmarking of 50 nm features in thermal nanoimprint. J. Vac. Sci. Technol. B25(6) (2007), pp. 2373–2378.

VIII Alternative Lithography: Unleashing the potentials of Nanotechnology, edited by C. M. Sotomayor-Torres, University of Wuppertal: Ahopelto, J. and Haatainen, T.: In chapter 6 “Step and Stamp Imprint Lithography”, Kluwer Academic/Plenum Publishers, New York 2003. Pp. 103–115.

Author's contribution

In Publication I, the imprint experiments, including imprint parameter optimization and analysis of the results using AFM and SEM, were carried out by the author. The author also modified the interface of the flip chip bonder to make it suitable for sequential imprinting. The manuscript was written by the author.

In Publication II, the experimental work, including the imprint experiments and dry etching of the samples as well as the analysis of the results, was carried out by the author. The manuscript was written by the author.

In Publication III, the author planned the experimental work with the co-authors. The TiW/Cu sputtering process was mainly developed by T. Riekkinen, and the electroplating process was developed by P. Majander. The author participated in the experimental work and carried out all the SEM and AFM analyses of the samples. The author finalized the manuscript together with the co-authors.

In Publication IV, the author participated in the planning of the experimental work with the co-authors. The AFM analysis of the experiment was carried out by the author. The author participated in finalizing the manuscript together with the co-authors.

In Publications V and VI, the author planned the experimental work. The experimental work and analysis were carried out by the author, and the manuscript was written by the author.

In Publication VII, the author participated in the planning of the experimental work and carried out the step and repeat imprint tests in the experiment. The author participated in preparing the manuscript together with the co-authors.

In Publication VIII, the planning, experimental work, and analysis of the results were carried out by the author. The manuscript was finalized together with Prof. Jouni Ahopelto.

Related publications

IX Merino, S., Schift, H., Retolaza, A. and Haatainen, T. The use of automatic demolding in nanoimprint lithography processes. Microelectron. Eng. 84 (2007), pp. 958–962.

X Mäkelä, T., Haatainen, T., Ahopelto, J. and Isotalo, H. Imprinted electrically conductive patterns from a polyaniline blend. J. Vac. Sci. Technol. B19(2) (2001), pp. 487–489.

XI Mäkelä, T., Haatainen, T., Ahopelto, J. and Isotalo, J. Imprinted electrically conductive polyaniline blends. Synth. Met. 121 (2001), pp. 1309–1310.

XII Mäkelä, T., Haatainen, T., Majander, P. and Ahopelto, J. Continuous roll to roll nanoimprinting of inherently conducting polyaniline. Microelectron. Eng. 84 (2007), pp. 877–879.

Contents

Abstract 3

Tiivistelmä 4

Preface 5

List of publications 7

Author's contribution 9

Related publications 10

List of symbols and abbreviations 13

1. Introduction 15
   - 1.1 The objective of the thesis 16

2. Basics of nanoimprint lithography 18
   - 2.1 The imprint parameters 19
   - 2.2 Residual layer 21
   - 2.3 Thermoplastic materials 22
   - 2.4 Imprint molds 23
   - 2.5 Antiadhesion treatment 24

3. Stamp fabrication by imprinting 26
   - 3.1 Sequential imprinting method 28
   - 3.2 Imprint tools 31
     - 3.2.1 Imprint machines 31
     - 3.2.2 Stamp holder 34
   - 3.3 Evaluation methods 35
     - 3.3.1 Optical microscopy 35
     - 3.3.2 Scanning electron microscopy (SEM) 36
     - 3.3.3 Atomic force microscopy (AFM) 36
     - 3.3.4 Reflectometry 36
   - 3.4 Fabricated stamps 37
     - 3.4.1 Replication of silicon stamps 37

3.4.2 Bendable nickel stamps 46
3.4.3 UV-NIL stamps 52

4. Summary and discussion 59

References 61

Appendices
Papers I–VIII

Papers I–VIII are not included in the PDF version.
Please order the printed version to get the complete publication
(http://www.vtt.fi/publications/index.jsp).

List of symbols and abbreviations

AFM	Atomic force microscope
CD	Critical dimensions
DUV	Deep ultra violet
EBL	Electron beam lithography
EUV	Extreme ultra violet
HEL	Hot embossing lithography
HSQ	Hydrogen silsesquioxane
MAA	Methacrylic acid
MMA	Methyl-methacrylate
NIL	Nanoimprint lithography
PBM	Aromatic acrylate-base polymer with glass temperature of 49 °C
PET	Polyethylene terephthalate
PHS	Polyhydroxystyrene
PMMA	Polymethylmetacrylate
PPM	Aromatic acrylate-based polymer with glass temperature of 107 °C
RIE	Reactive ion etcher
SEM	Scanning electron microscope
SFIL	Step and flash imprint lithography
SiC	Silicon carbide
SSIL	Step and stamp imprint lithography
T_g	Glass transition temperature
UV	Ultraviolet
UV-NIL	Ultraviolet nanoimprint lithography
UV-SSIL	Ultraviolet step and stamp imprint lithography
η	Viscosity

1. Introduction

The semiconductor industry has traditionally relied on optical lithography, which has been an ideal tool for volume manufacturing. The requirements for mass manufacturing include resolution, overlay accuracy, and economics [1]. The miniaturization of devices and integrated circuits beyond the capability of UV lithography sets high demands for equipment and increases costs, while processing becomes more complicated. The limits of optical lithography have been pushed many times to meet the requirements that have been encountered [2, 3]. Optical lithography has been under constant development and has already reached sub-50 nm resolution. The next step is extreme ultraviolet lithography (EUV) [4, 5], which is expected to take the resolution below 20 nm. Alternative methods for optical lithography for patterning sub-micron-scale features have been searched for in X-ray lithography [6], ion beam lithography [7], and electron beam lithography (EBL) [8]. Nanoimprint lithography (NIL), which was introduced in 1995 by Stephen Chou, was quickly recognized as a potential candidate for post-optical lithography [9]. The advantage of NIL is that it can offer high resolution without the need for imaging optics or complex light sources, as in the case of the other alternatives [10].

After a demonstration of sub-10-nm features, NIL was expected to become a next-generation lithography tool for many applications, replacing optical lithography [11, 12]. Large-area nanoimprinting can be faster than sequential electron beam lithography and simpler than X-ray lithography. Soon after Chou's invention, the interest in imprint lithography grew rapidly in many research laboratories. Previously published results demonstrate that the resolution of imprint lithography is not an obstacle. The roadblocks on the way to efficient production are overlay accuracy and throughput [13]. The benefits of the method overcome the roadblocks, for example, imprinting can be used to pattern functional structures in polymers, and this can be exploited in, for example, biotechnology and

photonics [14]. The fabrication of stamps with nanoscale features is slow with the current methods, however, and can create a bottleneck in the NIL, when broken and contaminated stamps need to be replaced. There is a need for a stamp replication and surface enlargement method that is affordable and sufficiently fast compared with, for example, EBL.

1.1 The objective of the thesis

Nanoimprint lithography is a promising candidate for a low-cost, high-throughput method of fabricating nanometer-scale features. There are different variations of NIL, for example, the wafer-scale, and the step and repeat method based on mechanical deformation of the polymer, which can be thermoplastic, or thermally or UV curable. Common to all these methods is that they rely on a patterned mold carrying nanoscale protrusions brought into contact with the polymer. The physical contact gives rise to a risk of contamination or breakage of the mold, and the availability of affordable spare molds is therefore important.

The bottleneck is the availability of the molds, which are still mainly fabricated using clean room nanofabrication processing methods. Patterning of a large mold is time consuming and expensive using, for example, e-beam lithography and dry etching. The lifetime of the stamp can be increased by reserving the original mold as a master for a stamp-copying process.

Economical and high volume manufacturing of submicron scale features in microelectronics and optics require low-cost molds. The aim of this study was to develop a method for economical stamp fabrication. Sequential imprinting, used in this work, can offer a low-cost method to pattern large-area stamps or a number of copies from an original master.

This thesis focuses on developing large-scale pattern transfer for stamp fabrication by thermal NIL. The stamp replication is established on patterning thermoplastic polymers using silicon molds that were patterned using UV or electron beam lithography and dry etching. This thesis is divided into two parts: an introduction and an overview of imprint lithography in Chapters 1 and 2, and an experimental part in Chapter 3 covering results and work published in journals included in the thesis. The experimental work reported in this thesis covers the development of Step and Stamp Imprint Lithography (SSIL). Novel large scale pattern transfer into silicon substrate, fabrication of bendable metal stamp with 100 nm features and fabrication of UV stamp with 50 nm features have been demonstrated. The tools and evaluation methods are also reported. The pattern

transfer onto silicon, which enables the fabrication of silicon stamps [I, II, VII, VIII], is described in Section 3.4.1. Section 3.4.2 deals with the fabrication of flexible metal stamps for roll-to-roll nanoimprinting [III, IV]. The bendable metal stamps are used in the roll-to-roll nanoimprinting process, which is also available at the VTT's laboratory. Section 3.4.3 reports on a novel method to fabricate transparent polymer stamps for the sequential UV imprinting process, which is also available at the VTT's facilities [V, VI]. The research has been carried out in the Nanoelectronics Team at the VTT Technical Research Centre of Finland.

2. Basics of nanoimprint lithography

Nanoimprint lithography is, basically, mechanical deformation of a polymer using pressure and elevated temperature. Imprinting requires three basic components: a patterned mold, printable material, and equipment to control pressure and temperature, with the ability to bring the mold into parallel contact with the substrate. A mold with a featured surface is used to transfer patterns onto the thermoplastic polymer. The temperature of the mold is raised above the glass transition temperature of the polymer before applying pressure. The patterns in the mold are copied into polymers with opposite polarity. The mold is allowed to cool down below the glass transition temperature before separation. The schematic of the process is shown in Figure 1.

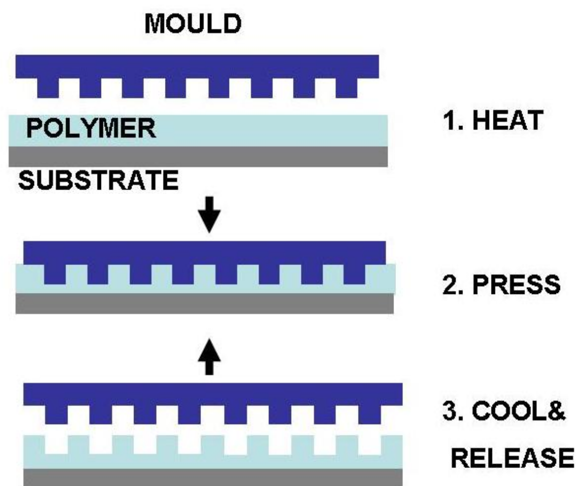

Figure 1. Schematic of the nanoimprint lithography process. The thickness contrast is created in the resist by imprinting (1). The pressure is maintained until the polymer flow fills the cavities of the mold (2). The mold and substrate are cooled below the glass transition temperature and separated (3).

Different imprint methods, such as parallel-scale nanoimprinting, thermal step and repeat, UV step and flash, and microcontact printing, have been used for a number of applications [15]. Examples of applications already realized by imprinting are high aspect ratio MEMS structures [16], photonic crystals [17, 18], sub-wavelength periodic structures [19], metal-semiconductor-metal photodetectors [20], field emitters from organic materials [21], field effect transistors [22], interdigitated electrodes [23], data storage disks [24, 25], microrings [26], and 3-D T-gate and air bridge structures [27].

2.1 The imprint parameters

In optical lithography, the sensitivity of the resist defines the exposure time and affects the throughput. In imprint lithography, the molding time corresponds to the exposure time and requires understanding of material rheology. During imprinting at elevated temperatures, the polymer melt is forced to flow into mold cavities by pressing the mold against the substrate. After a complete cavity fill, the mold and the substrate are cooled below T_g to obtain mechanically stable structures. In this state, the features in the polymer are rigid enough to survive the separation from the mold. The throughput is related to the processing time needed for heating, cooling, and the cavity fill completion time. These times are related to the polymer flow properties, which, in turn, are related to the temperature. The limits for the suitable temperature range are set by the thermal stability of the polymer.

At temperatures below T_g, the deformation takes place due to elongation of the atomic distances, and this deformation is elastic. Young's modulus below T_g is high. In this temperature range, the deformation is very small. In order to obtain melt state with proper flow properties, the polymer is heated above its T_g. When the polymer is heated above T_g, the modulus drops several orders of magnitude, while local motion of chain segments takes place. At this temperature range, the chains are still fixed by the network of entanglements. Above T_g, there is a rubber-elastic region where chain segment extension between fixed points allows relatively large deformation. The modulus is nearly constant in this region, and deformation is recovered when pressure is released. When the temperature is increased sufficiently, the viscous flow region is reached. An entire chain can move in this regime, and polymer flow takes place by chain sliding. The viscosity and modulus are further reduced, and deformation is irreversible. The time needed to complete the cavity fill can be estimated using an equation derived

from the two-dimensional squeeze flow theory. In the squeeze flow model, the material is assumed to be purely viscous, and elastic behavior is neglected [28, 29]. The cavity fill time t_f is solved by calculating the time required to displace the amount of polymer with a stamp protrusion of total width *S*; see Figure 2.

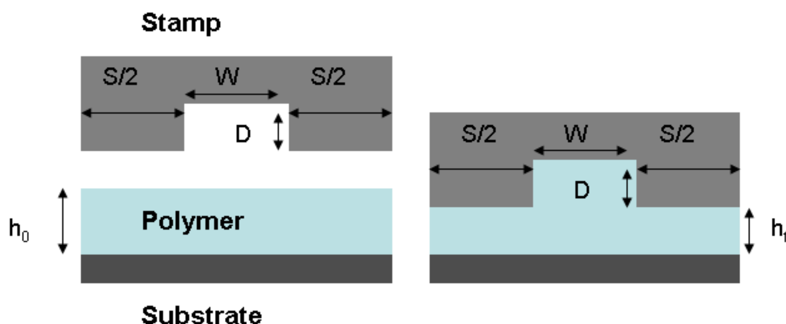

Figure 2. Thickness of the polymer layer before imprinting (left) and after the cavity fill is complete (right).

The assumption in the following equation is that the liquid is purely viscous, the adhesion of the polymer is ideal at the surfaces, the polymer melt is incompressible and $S >> h(t)$, no air is trapped in the cavities, and there is no stick-slip effect at the interfaces. The imprint time is then given by following equation:

$$t_f = \frac{\eta_0 S^2}{2p}\left(\frac{1}{h_f^2} - \frac{1}{h_0^2}\right) \quad (1)$$

In equation (1), h_0 is the initial thickness of the polymer film, h_f is the thickness of the residual film (the final height of the film when the cavity has been filled), η_0 is the viscosity of the polymer, p is the imprint pressure, and *S* is the width of stamp protrusion.

Equation (1) shows that in order to decrease the imprint time, the viscosity must be decreased and the imprint pressure increased. A higher film thickness and lower ratio of cavity volume to stamp width decreases the imprint time. Usually, the film thickness is optimized to the stamp feature height in order to minimize the final film thickness and obtain the minimum residual layer thickness for the subsequent pattern transfer. The theory ignores the more complex flow in the complicated stamp geometries, capillary effects, surface tension, elastic response of the polymer, forming of the mound surface [30, 31], shear

rate effects [32, 33], and mold deformation due to mechanical stress, such as tension, compression, flexion, and torsion [34, 35, 36]. At imprint temperatures, the polymer is a high viscosity liquid that responds to applied pressure by instant elastic deformation within the typical relaxation time of the material and flow at a rate depending on the viscosity. The relaxation time and viscosity depend on the temperature, and they decrease when the temperature increases. The time-temperature relation is described by the Williams-Landel-Ferry (WLF) equation [31, 37]:

$$\log\frac{\tau}{\tau_0} = \log\frac{\eta}{\eta_0} = \frac{-C_1(T-T_0)}{C_2+(T-T_0)} \tag{2}$$

In equation (2), τ is the time constant, η is the viscosity, and T is the absolute temperature. The index *0* denotes the values at a reference temperature T_0. C_1 and C_2 are constants at the reference temperature. Due to the exponential influence of the temperature on the viscosity, it is more efficient to increase the temperature than the time. The effect of the increased pressure is more complex due to the shear thinning effect. At temperatures that are not high enough above T_g, the differences in polymer flow rate between dense and isolated structures can result in non-uniform residual thickness [38]. On the other hand, at high temperatures, low viscosity may result in self-assembly of the polymer. Scheer et al. [39] have shown that the best imprint results are achieved at temperatures at which viscosity is approximately 10^6 Pas. In SSIL, the small size of the stamp enables high imprint pressures, reducing the imprint time considerably compared with the parallel wafer-scale processes under similar temperature conditions.

2.2 Residual layer

The uniformity of the residual is important in situations in which the imprint resist is used as a mask in subsequent lithographic steps. The residual can be optimized by choosing the initial film thickness according to the local polymer volume needed for flow and filling the stamp cavities [40]. It is quite easy to calculate it for simple and periodic structures, but when complex stamp geometries are involved, the calculations become complicated. Different numerical methods have been used to calculate polymer flow during imprinting. Hirai et al. [41, 42] have studied pressure and resist thickness dependency using the finite element method. Kehagias et al. [43] have used the coarse-grain method to calculate simultaneous resist viscous flow and stamp/substrate deformation during

imprinting. Young [44] has analyzed polymer flow in nanoimprinting using a simulation model based on the viscous model. Sirotkin et al. [45] have modeled resist flow by the coarse-grain method derived from the 3D Navier-Stokes equations. Rowland et al [46] have studied the impact of film thickness and cavity size on polymer flow using a Galerkin finite element program. Scheer et al. [47] studied elastic recovery in squeeze-flow-dominated thermal imprint using commercially available MARC software based on the Moony-Rivlin model.

The imprinted polymer can be used as a mask after removing the residual layer. An anisotropic dry etching step is needed to reduce the resist layer by at least the thickness of the residual to expose the substrate. In an ideal process, the resist layer thickness is reduced without affecting the profile of the features. In practice, the residual is typically removed in an RIE process using O_2 plasma [9]. The thickness contrast should be high and the residual layer as thin as possible to maintain the fidelity of imprinted features during the dry etch process. The dry etch process is not needed in the partial cavity filling method, which is able to produce a very thin residual layer [48, 49]. In this method, the residual thickness is minimized using a stamp with protrusions higher than the initial thickness of the resist. As a result, the residual film is very thin, and the metal layer can be sputtered directly on the resist. The drawback of this method is the elastic recovery of large structures [50]. Another approach that can avoid elastic recovery is to exploit the multilayer resist method and still maintain a high thickness contrast [51, 52, 53, 54]. On the other hand, a thick residual layer has an advantage: it is like a soft barrier between the stamp and the hard substrate, thus protecting the stamp from wear, which is especially important on patterning non-flat surfaces by NIL [55].

2.3 Thermoplastic materials

Imprint polymers can be divided into thermoplastic, thermally curing, and photochemically curing materials. Thermoplastic polymers become soft above T_g, and they can be molded repeatedly. Thermally curing polymers start to cross-link at elevated temperatures, leading to high thermal stability, thus preventing re-printing. Prepolymers of photochemically curing polymers are low-viscosity liquids enabling a short imprint time and low residual layer at room temperature. This is cured by UV irradiation, leading to a mechanically and chemically stable polymer. Regardless of material, there are some general requirements for NIL, for example, high thickness uniformity, adhesion to the substrate, low viscosity

during imprinting, and high pattern transition fidelity. Special physical properties defined by an application have been a driving force to develop new materials.

One of the first materials used for thermal imprinting is poly-methyl methacrylate (PMMA), known as an electron beam resist. PMMA possesses many properties that make it suitable for nanoimprint lithography, for example, small pressure and temperature shrinkage coefficients [56, 57]. Experimental work has revealed that the temperature is the dominant parameter to achieve adequate flow for the imprint process [58]. The characteristics of the polymer limit the control of the process temperature and thus the polymer flow. Extended control has led to the tailoring of characteristics of the polymer for imprint purposes. For example, the T_g of the resist has been adjusted by varying the composition of the co-polymers of methyl-metacrylate (MMA) and methacrylic acid (MAA) [59]. The PHS-based electron beam resist NEB-22 has shown high resolution and good plasma etch selectivity to silicon [60]. Aromatic polymers (PPM, PBM) developed for imprint purposes offer high dry etch resistance with tunable T_g by varying the number of aromatic groups that are incorporated [61, 62, 63]. The bulk material can be patterned by thermal imprinting without the resist mask. The resistless method has been used in patterning, for example, polymer cellulose acetate [64], PET [65], polycarbonate [66], glass [67], and silicon [68].

2.4 Imprint molds

Imprint lithography relies on a mold carrying the patterns to be replicated. The mold is analogous to the photo mask in the UV lithography. Being a direct contact technique, the resolution depends directly on the size and quality of the mold. The resolution of the mold, in turn, depends on the mask technology providing the original patterns. The first generation mold, fabricated using existing mask technology, is usually called a master stamp.

There is a variety of methods and materials to fabricate nanoimprint masters. UV and electron-beam lithography are the most common methods to fabricate masters. They are common patterning methods in the semiconductor industry and research laboratories. Nowadays, the resolution of UV lithography enables patterning of polymers on a submicron scale. The resolution of UV lithography has been improved, but with increasingly complicated lithography processes. Where available, electron beam lithography is used to achieve a sub-50-nm re-

gime. Nowadays, e-beam facilities are available in almost every semiconductor research laboratory. A standard scanning electron microscope (SEM) can be converted into a lithography tool with reasonable investment in accessories, including software and beam control hardware.

The material of the mold is selected considering the following properties: hardness and compatibility with conventional microfabrication processes, and the thermal expansion coefficient. A significant difference in thermal expansion between the stamp and the substrate can result in stress or pattern distortion during the cooling period, because thermal imprinting is typically carried out at temperatures of 100–200 °C. Silicon has been used widely for stamp fabrication, because it fulfills the above requirements, and the knowledge and equipment for processing Si are commonly available in research laboratories.

Electron beam lithography and dry etching are a typical combination to pattern, for example, silicon-based (Si, SiO_2, Si_xN_y) masters [69, 70, 71, 72]. Another direct writing method is focused ion beam (FIB) milling, which is used to create 3D features [73, 74] directly.

Nickel is interesting as a stamp material, offering high mechanical strength and durability [75, 76]. Polymer-on-silicon or full polymer stamps have been fabricated, patterning cross-linking polymers by direct e-beam writing or embossing [77, 78, 79]. Hydrogen silsesquioxane (HSQ) is an electron beam resist showing high lateral resolution and good mechanical properties for stamp fabrication [80]. Epoxy resin and PDMS have been used in a casting process that relies on a patterned mold [81, 82].

2.5 Antiadhesion treatment

The high density of nanoscale patterning in the mold increases the total surface in contact with the resist, showing a tendency to improve polymer adhesion to the resist. The increased adhesion leads to the polymer sticking to the mold and to the tear-off of the resist during separation. The resist-to-stamp sticking is prevented by applying low-surface tension coating, thus reducing the surface energy of the mold. The anti-adhesion layer can be applied to the stamp plasma deposition or to the wet method.

Teflon is a chemically inert polymer with low surface energy and good anti-wetting properties. Teflon-like films can be applied to the stamp surface either by the plasma deposition process using C_nF_m molecules as a polymer precursor supply [83, 84] or by a sputtering process using a Teflon target [85].

Chlorosilanes can be used to create Self-Assembled Monolayers (SAM) on silicon. Chlorosilanes react spontaneously with hydroxylated silicon or silicon dioxide surfaces, forming a non-polar surface instead of the polar SiO_x, thereby increasing the surface energy and the contact angle. The molecules can be applied to the substrate by the vapor phase or liquid deposition. Ttridecafluoro-(1,1,2,2)-tetrahydrooctyl-trichlorosilane (TFS or F_{13}-TCS) is widely used as an antiadhesive layer [86, 87, 88]. The contact angle of water on silicon dioxide has been shown to increase from 64.5° for an untreated stamp to 105° for a SAM-treated stamp, correspondingly [89]. The contact angle of water on silicon has been shown to increase from 22.2° to 95° with perfluorooctyltrichlorosilane treatment [90].

3. Stamp fabrication by imprinting

In the first experiments, the imprints were performed in a single step process using a stamp with the maximum size of a few square centimeters. Industry requires large-scale imprinting, and there are two approaches to reach this goal: the wafer-scale parallel process and the sequential process. In the parallel method, the substrate is patterned with a stamp of the same size. The first experiments were conducted using simple systems. For the wafer-scale imprinting [IX], just a hydraulic press can be used. The more sophisticated systems are able to perform stamp-to-substrate alignment. In the wafer-size stamps, the nanometer-scale features were typically distributed over a few locations on the wafer. In the sequential method, a small master (Figure 3) is patterned with nanometer-scale features (Figure 4) by e-beam and replicated over large areas by sequential imprinting (Figure 5).

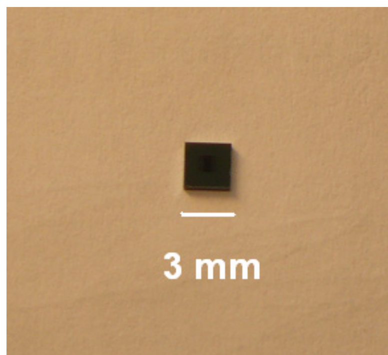

Figure 3. Silicon master with an area 1 mm x 1 mm, patterned by electron beam lithography in the center. The pattern consists of a grating with sub-micron lines with a pitch of 500 nm.

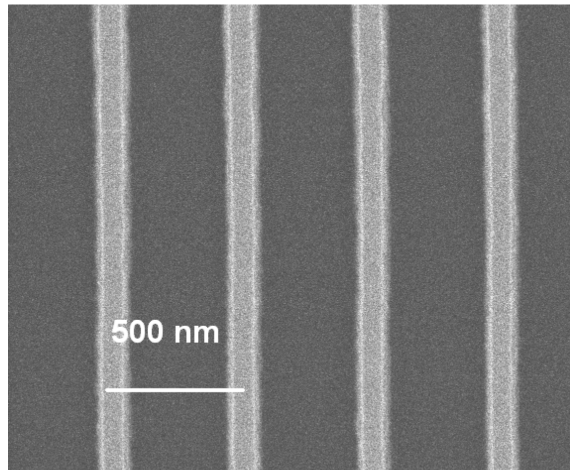

Figure 4. SEM micrograph of sub-200-nm grating of the silicon stamp shown in Figure 3.

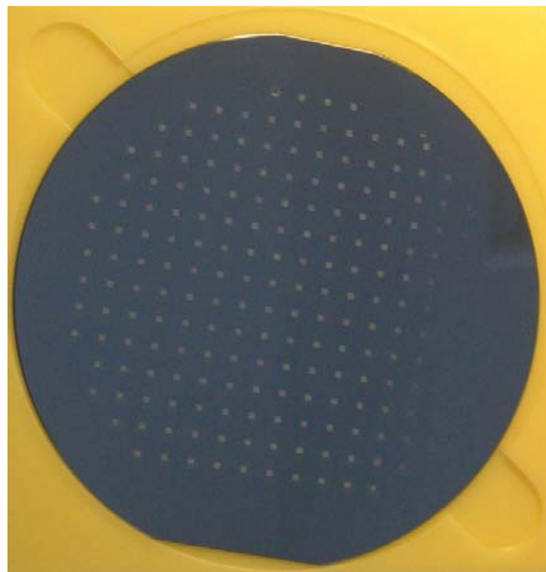

Figure 5. Large-scale imprinting by SSIL. Two hundred imprints on a 100-mm silicon wafer using a stamp with a 1 mm x 1 mm area covered by a nanometer-scale grating.

3.1 Sequential imprinting method

Papers I, II and VIII describes the use of a commercial flip chip bonder for performing Step and Stamp Imprint Lithography (SSIL) experiments. The experiments included optimizing the imprint parameters (pressure, temperature and time) and analyzing the uniformity of the transferred patterns. The system mimics the operation of the optical stepper, exposing the substrate chip by chip. The stamp is used like a reticle in an optical stepper to pattern one chip at a time. In a thermal sequential approach, the requirements for an imprint apparatus are heating and pressing capabilities with the possibility of moving and aligning the stamp with respect to the substrate. A patterned mold or “stamp” surface is prepared using advanced Si fabrication technology, for example, electron beam lithography that enables the writing of small patterns onto the resist and finally transfers patterns into the substrate by dry etching. The stamp is pressed into a thin polymer film spun onto a substrate. The polymer is imprinted at elevated temperatures, at which the viscosity is relatively low and the polymer is able to flow under pressure. The stamp is cooled below the glass transition temperature before releasing the pressure and separation. The stamp is then moved to the next site and the imprinting process is repeated. The process is presented schematically in Figure 6.

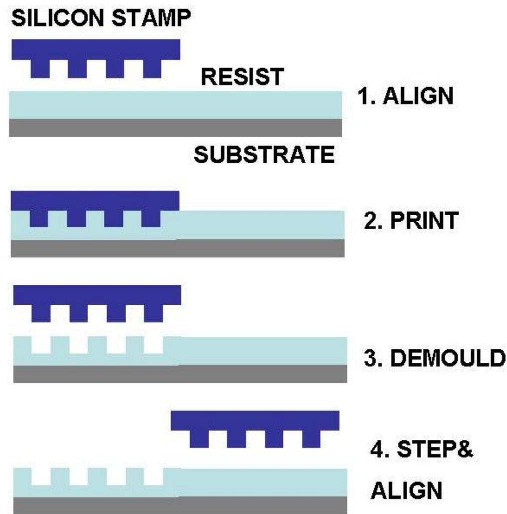

Figure 6. Schematic of step and stamp imprint lithography: (1) The stamp is aligned to the substrate. (2) The stamp is heated and pressed into the resist. (3) The stamp is cooled and demolded. (4) The sequence is repeated in the new location.

SSIL is a relatively flexible method that can be applied to a large area and multi-layer patterning. In addition to wafer patterning, SSIL can be used to pattern different substrate materials with a variety of shapes and thicknesses. In the mix and match approach, imprinting and conventional UV lithography can be combined to merge the advantages of both technologies.

In SSIL, the substrate is imprinted row by row (Figure 7). The task differs from the parallel imprint method by repetitive temperature cycling. In the sequential method, the heating and cooling cycles are repeated for each imprint. Successful patterning requires the patterns to survive the thermal cycling without profile deformation and loss of dimension control.

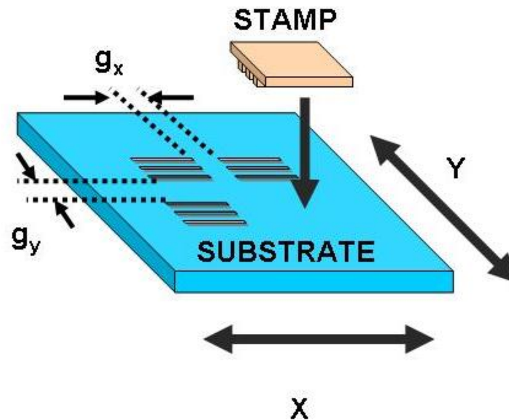

Figure 7. Patterning of a matrix by stepping the substrate chuck in the xy direction. The gap (g_x and g_y) between imprints is typically >100 μm.

The imprint process requires proper material and optimized parameters (temperature, pressure, and time). The optimization of the parameters was performed by studying the effect of the altered parameters on the profile of the imprinted features [I, II, VIII]. The profile and the residual layer of imprinted features were evaluated by atomic force microscopy, optical microscopy, reflectometry, and electron microscopy.

The force and temperature profiles of an imprint cycle are presented schematically in Figure 8. The solid line in Figure 8 represents the temperature of the stamp, and the dotted line shows the pressure applied to the stamp. The glass transition temperature is marked with a horizontal line. In the first step, the stamp is heated above the glass transition temperature of the polymer. The stamp is then pressed into the polymer. The force is applied to the stamp for the period needed for the resist to flow and accommodate the shape of the stamp protrusions. The stamp is cooled down below the glass transition temperature before separation.

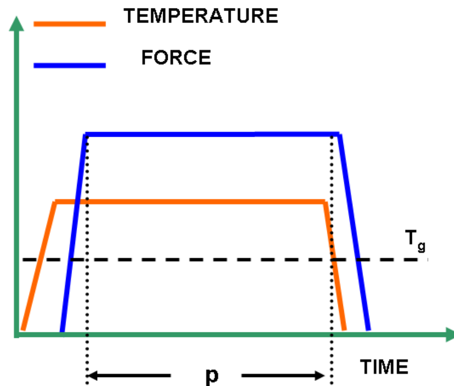

Figure 8. Force and temperature profile of an imprint cycle. The stamp is first heated above the glass transition temperature of the polymer and then pressed against the polymer. The force is applied to the stamp for the period, p, needed for the resist to flow and accommodate the shape of the stamp protrusions. The stamp is cooled down below the glass transition temperature before demolding.

The stamp temperature, imprint pressure, and imprint time must be chosen by the material parameters of the resist and the feature sizes and topography of the mold. The parameter window for sequential thermal imprinting is narrower than for the parallel method, which is used to pattern a whole wafer in a single press. In a sequential method, thermal cycling makes process control more challenging to prevent pattern deterioration during the process.

3.2 Imprint tools

3.2.1 Imprint machines

The first imprint tests were carried out using a Karl Suss FC150 Flip Chip Bonder (shown in Figure 9), which was found to be suitable for testing the sequential imprint concept without hardware modification. In a bonding mode, in which the machine is typically used, the chip is aligned with the substrate chip and bonded onto it. After bonding, the machine fetches the next chip and continues bonding. The imprint process proceeds in a similar manner. In the sequential imprint mode, the machine fetches the stamp, runs the temperature and force control cycle, and continues by moving the substrate chuck after each imprint.

Figure 9. Photograph of an FC150 Flip Chip Bonder in a clean room.

The key elements of the imprint machine are the mobile xy chuck, the imprint arm, and the alignment/collimation optics shown in Figure 10. The stamp is attached to a SiC plate of the bonding arm with a high-temperature silicone adhesive. The elasticity of the adhesive helps to level the stamp with the substrate when it is in contact with it. The substrate chuck was also made of SiC. The machine was equipped with a motorized high-resolution xy stage. The resolution of the stage is 0.1 μm. The autocollimator is capable of leveling the stamp with the substrate with a resolution of 20 μrad. The force, which the bonding arm applies to the stamp, is adjustable within the range 0.3–500 N. Both the arm and the chuck temperature can be controlled separately from room temperature up to 450 ^{o}C. The system can be programmed to perform sequential step and stamp imprinting.

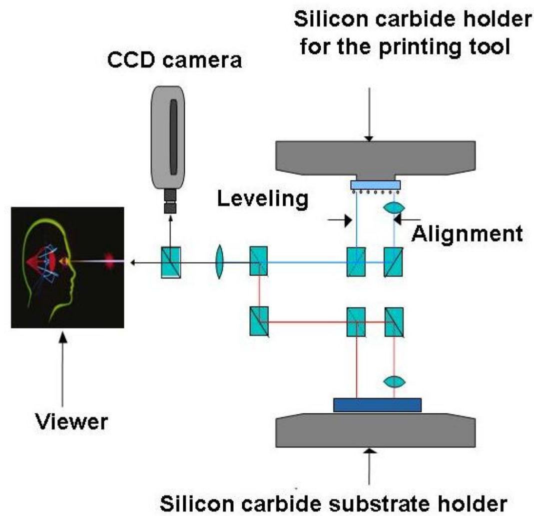

Figure 10. Schematic of the alignment/collimation optics, stamp, and substrate holder of the FC150 [I].

The NanoimPrinting Stepper NPS300 (shown in Figure 11) was developed in collaboration between VTT and S.E.T SAS [91] (formerly Suss Microtec) using experience collected from early imprint experiments with the FC150. The author participated in several discussions with manufacturers' representatives, supplying feedback during the planning and testing of the prototype. The emphasis was on the stamp-to-substrate parallelism mechanism, collimation optics, stamp size, and handling, as well as pressure and temperature control. The machine is designed for imprint lithography and addressing R&D requirements as well as production needs. The set-up of the system allows automatic, full wafer imprint, with an alignment capability. The main modules of the machine are a high-accuracy alignment stage, a microscope for alignment, and an imprinting arm. The following parameters can be controlled via software: stamp-to-wafer leveling, alignment, force, and temperature profiles. The stamp is aligned to the substrate using a microscope. The parallelism of the optical axes during movement is secured by an air-bearing xy-optics stage. A built-in autocollimator performs the stamp-to-substrate pre-leveling within 20-µrad accuracy using a motorized ball cup system. The self-leveling system uses a flexure stage supplement to reach two orders better parallelism. The imprinting arm is attached to the upper granite bridge of the machine, which also supports the optics stage. The arm's

vertical movement is controlled by a DC motor. The force profile during the imprint cycle is monitored and controlled using a closed-loop system with force sensors integrated into the imprint arm. The substrate chuck is heated using halogen lamps located under the optical, polished SiC top plate holding the wafer by vacuum. The imprinting arm includes ceramic heaters in the back of the optical, polished silicon carbide stamp holder, which is secured by vacuum. Both of the chucks are equipped with water cooling to maintain the housing at room temperature to avoid thermal drift.

Figure 11. Photograph of the NPS300 nanoimprinting stepper in a clean room.

3.2.2 Stamp holder

In the present work, the SSIL stamp material is silicon and its size is a few millimeters. The maximum size is limited to 50 mm × 50 mm, which is the size of the SiC plate used as a support for the stamp (Figure 12). The tool is designed to be replaceable and to be raised by vacuum. As the stamp is demolded automatically, it needs to be attached to the imprinting arm with a bond that is strong enough to overcome the adhesion force to the resist. The adhesive has to be thermally conductive and bear temperatures at least up to 200 °C. The Dow

Corning Q1-9226 is a high-temperature, two-component silicone adhesive that is mixed at a 1:1 ratio [92]. The mixture is cured at 150 °C for 30 minutes to reach the final strength. The stamps are patterned by either UV lithography or e-beam lithography depending on the resolution required. Submicron features are processed into silicon substrate using electron beam lithography and high-resolution e-beam resists. The developed e-beam resist is used as a mask for pattern transfer into silicon using the dry etching process. The patterned substrate is diced into chips that can be glued onto the SiC tool. The stamp can also be treated by an antiadhesion coating to prevent the resist from sticking to the stamp.

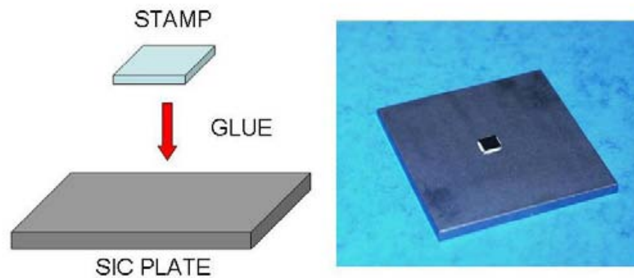

Figure 12. Schematic showing attachment of a stamp on a support tool by glueing (left) and a photograph of the SiC tool with a stamp glued on the top (right).

3.3 Evaluation methods

3.3.1 Optical microscopy

The optical microscope was used to obtain an overview evaluation of the imprinted sample. In bright field mode, the light microscope is capable of showing any rupture of the resist, which is an indication of possible resist-to-stamp sticking. The microscope was used in the dark field mode to search for particles, as a sign of contamination of the stamp or the substrate surface.

3.3.2 Scanning electron microscopy (SEM)

SEM was used to measure the surface and cross-section features with a size beyond the resolution of optical microscopy. In SEM, the specimen surface is imaged by scanning it with a beam of electrons. The electrons interact with the atoms near the surface of the specimen and produce a signal consisting of backscattered electrons. The electrons are collected in a detector, and the signal is transformed to image the surface topography of the specimen. The instrument used in the analysis of this work was the LEO1560 FE-SEM with a resolution of about 1 nm.

3.3.3 Atomic force microscopy (AFM)

The height and profile of the imprinted features are evaluated with an AFM in tapping mode.

The surface of the specimen is scanned by a sharp tip on a cantilever. The cantilever is silicon or silicon nitride, and the tip radius of curvature is a few nanometers. In tapping mode, the cantilever oscillates, barely touching the surface. The cantilever is forced to oscillate near its resonant frequency by a piezoelectric element in the tip holder. The amplitude of the oscillation is a few tens of nanometers. The feedback control detects the change in frequency or amplitude near the surface and moves the tip up and down to maintain the resonant frequency. Thus, the changes in resonant frequency can be used to measure the surface profile of the specimen. The instrument used in this work was the DI Dimension 3100 SPM.

3.3.4 Reflectometry

In this work, an optical reflectometer was used to define the initial thickness of the resist and the residual layer thickness of the imprinted features down to five micrometers.

A reflectometer is used to measure the thickness of optically transparent films. The intensity of the monochromatic reflected light depends on the film thickness due to interference. The computer-controlled grating monochromator and a photomultiplier tube detector measure the reflected spectrum from the bare reference wafer and the resist-coated sample. The computer analyzes the interference pattern and calculates the film thickness using a known refractive index and the

two measured spectra. The model of the instrument used in this work was Nano-Spec AFT 4150.

3.4 Fabricated stamps

There are different stamp types that can be categorized by the imprint method and size. The stamps can be divided into rigid stamps for thermal NIL for wafer-scale (parallel), large-area imprinting [93, 94, 95, 96], and small stamps for sequential imprinting [I, II, VII, VIII], bendable stamps for to roll-to-roll imprinting [III, IV], and transparent stamps for UV imprinting [V, VI].

3.4.1 Replication of silicon stamps

The different stamp types used in the experiments contained various structures defined by UV or electron beam lithography and were transferred onto the silicon substrate by dry etching. The patterns contained, for example, interdigitated fingers (400 nm) and large rectangular pads (100 µm), shown in Figure 13, dot arrays (400 nm, 1 µm, and 2 µm), shown in Figure 14, and periodic grating structures with 5 µm (Figure 15) and 200-nm-wide ridges, shown in Figure 16. Figure 17 shows 50-nm features of patterns by electron beam lithography. The small stamps were fabricated by dicing the substrate into small chips using a precision cutting tool. These chips were glued to SiC support tools by silicone adhesive. A summary of the stamps is presented in Table 1.

Table 1. Summary of the stamps used in the present work [I, II, VII, VIII].

Stamp identification	A	B	C	D
Stamp features	dots, pads, fingers	grating	grating	grating
Stamp size (mm^2)	5 × 5	3 × 3	3 × 3	20 × 20
Min. feature (nm)	400	5 000	200	50
Feature height (nm)	300	540	500	150

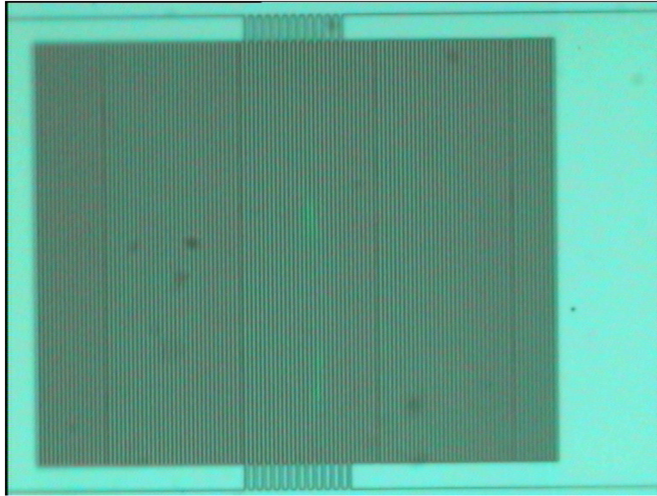

Figure 13. Optical micrograph of the 400-nm finger structures of stamp A.

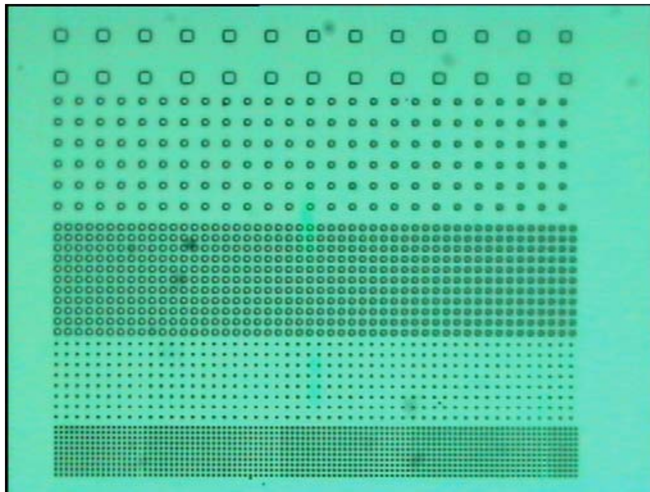

Figure 14. Dot arrays of 400-nm, 1-μm, and 2-μm dots of stamp A.

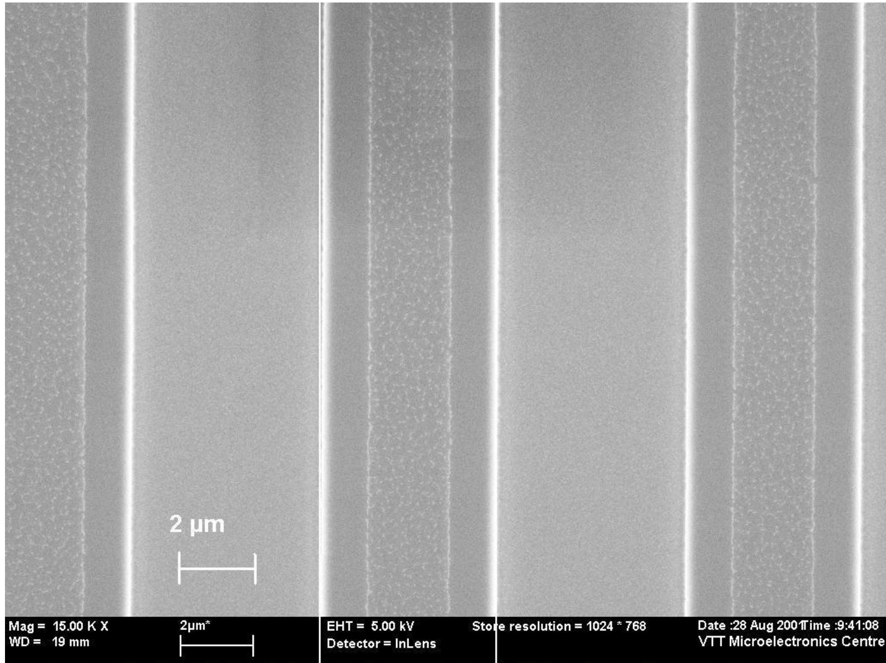

Figure 15. SEM micrograph of the 5-µm-wide grating features of stamp B.

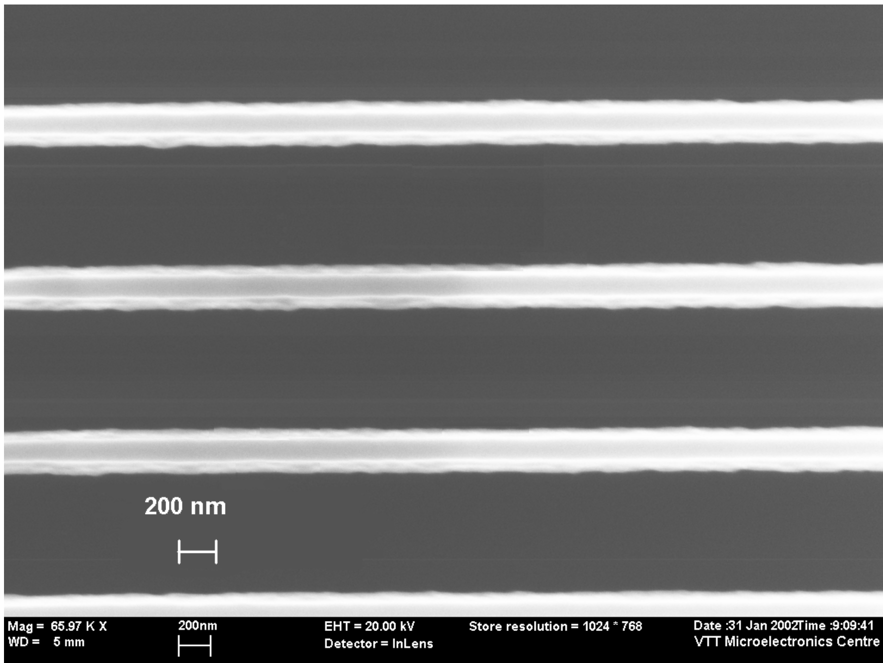

Figure 16. Ridges with 200-nm-wide features of stamp C.

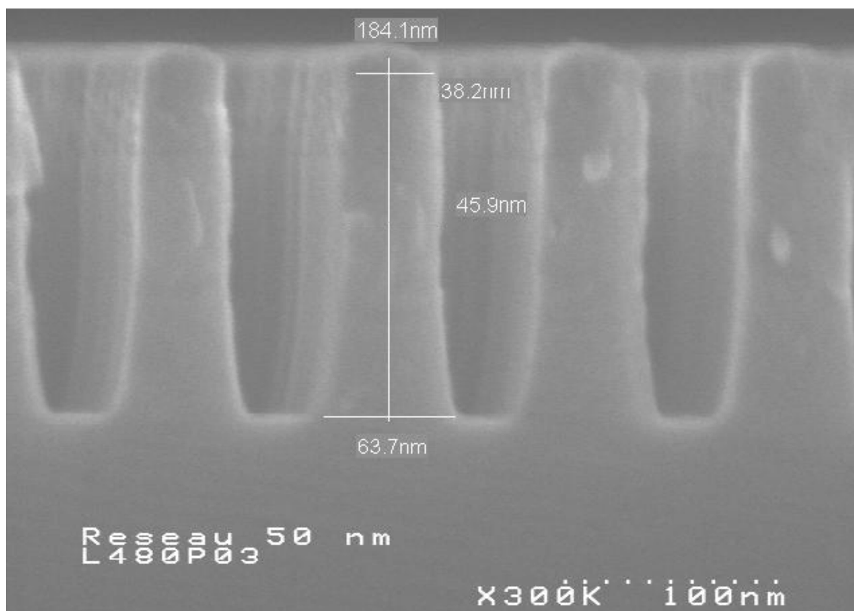

Figure 17. SEM micrograph of 50-nm features of stamp D [VII].

Methacrylate-based polymers containing aromatic components (PPM, mr-I 7000, mr-I 8000) were used in the experiments. The polymers were developed for thermal imprinting by the micro resist technology GmbH [97, 98]. Substrates were prepared by coating silicon wafers in a manual spinner and pre-baking on a hotplate. The wafer size was between 100 and 200 mm.

The proper imprinting parameters for each case were optimized by studying the effect of time, temperature, and force on the imprint quality. The imprint temperature was varied between 55 and 105 °C above T_g, and the force was varied from 5 N to 500 N. The imprint time was varied from a few seconds to 10 minutes. A summary of the optimized imprint parameters for different resists and stamps are shown in Table 2.

Table 2. Glass transition temperatures and typical imprint parameters of the resists used in the experiments.

Resist	T_g (°C)	Imprint temperature (°C)	Imprint time (min)	Imprint pressure (MPa)	Stamp
PPM	107	180	3	4.8	A
mr-I 7010	65	140	5	0.3	D
mr-I 7030	65	140	5	13	B
mr-I 8010	115	170	2	0.3	D
mr-I 8030	115	220	5	13	B

Figure 18 shows an optical micrograph of a two by three matrix consisting of six sequentially imprinted elements using stamp A. Each imprinted element consists of filter structures and dot arrays with sizes from 400 nm upwards. A detail from the boundary area with an imprinted dot array of 0.4-µm, 1-µm, and 2-µm features is shown in Figure 19.

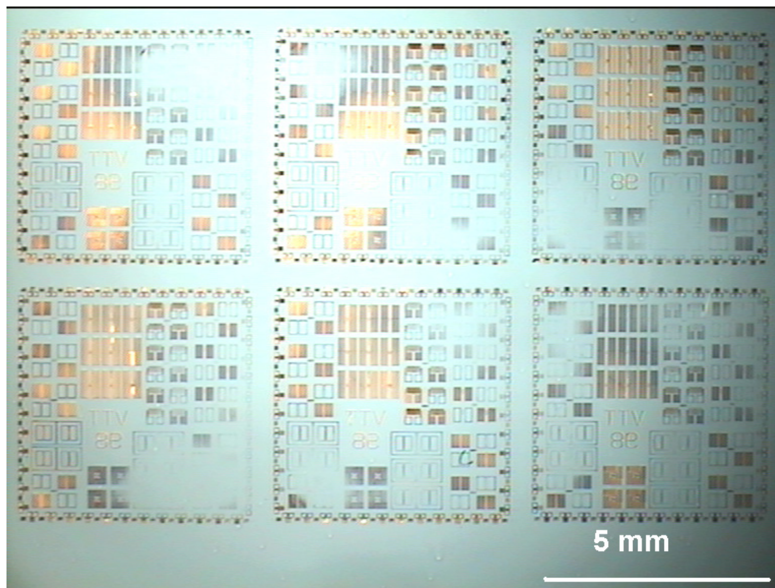

Figure 18. Optical micrograph of an imprinted two by three matrix in the thermoplastic polymer film. The gap between the adjacent imprinted elements is about 300 µm [I].

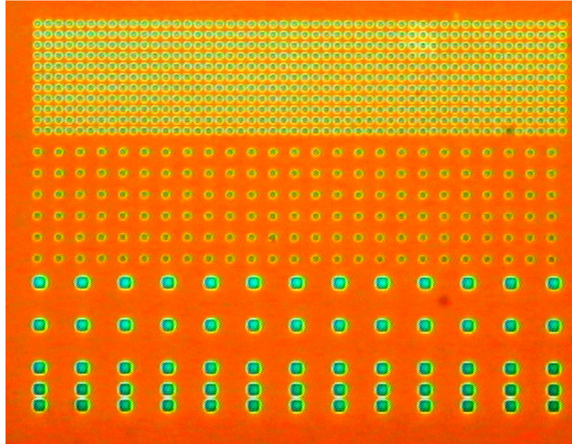

Figure 19. Optical micrograph of an imprinted dot array of 1-μm and 2-μm features [I].

Figure 20 shows a SEM micrograph of 50-nm features in a 101-nm-thick mr-I 8010 on a 200-mm silicon substrate. The features were imprinted at 170 °C with a force of 120 N, which corresponds to a pressure of 300 kPa. Due to the size (20 mm x 20 mm) of the stamp, the pressure remained moderate and imprints were not homogenous over the substrate [VII].

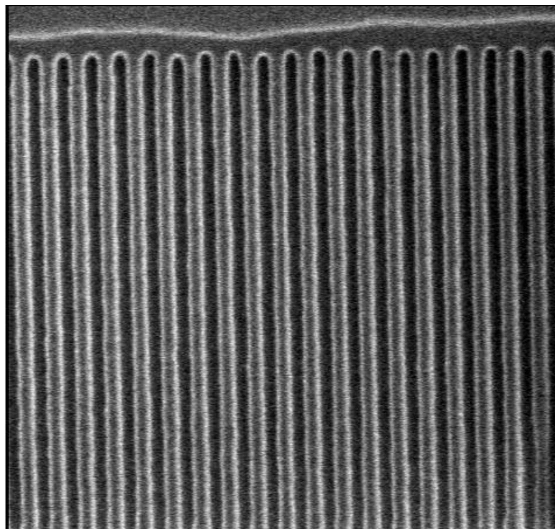

Figure 20. SEM micrograph of 50-nm features imprinted on a 101-nm-thick mr-I 8010 resist [VII].

Silicon stamps are fabricated using a dry etching process to transfer the imprinted patterns onto substrate. The resist can be used directly as an etch mask or a lift-off mask to fabricate a metal mask. First, the residual in the compressed area has to be removed [VIII]. Figure 21a shows a SEM micrograph of the residual layer with a thickness of 100 nm in the bottom of the 5-μm-wide imprinted trench. The residual was removed using oxygen plasma in the RIE at a pressure of 125 mTorr with RF power of 150 W at an etch rate of about 5 nm/s. Figure 21b shows the opening after residual removal.

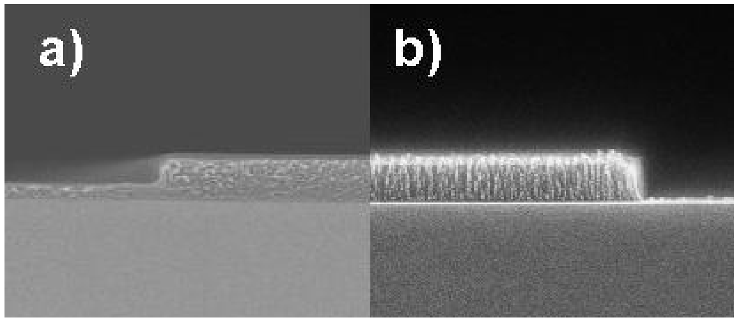

Figure 21. SEM micrograph of a residual layer of an imprinted mr-I 8030 film with an initial thickness of 345 nm a) and the film after the oxygen etch b).

The lift-off mask was fabricated by sputtering a 30-nm-thick layer of aluminum onto the imprinted resist. The resist was then dissolved in acetone in an ultrasonic bath. The features of the aluminum mask were transferred onto the silicon by a 10-minute CF_4/O_2 dry etch step. The height of the etched features was 200 nm. In Figure 22, an AFM image of the etched features in silicon is shown. The 5-μm features were replicated with adequate fidelity matching the feature dimensions of the stamp.

The replication quality of the submicron features was demonstrated by sputtering 30 nm of aluminum on the sample and removing the resist and the aluminum on top in a lift-off process. The 30-nm-thick aluminum film was used as an etch mask for RIE. Figure 23 shows the features on the silicon stamp and the 400-nm aluminum features respectively.

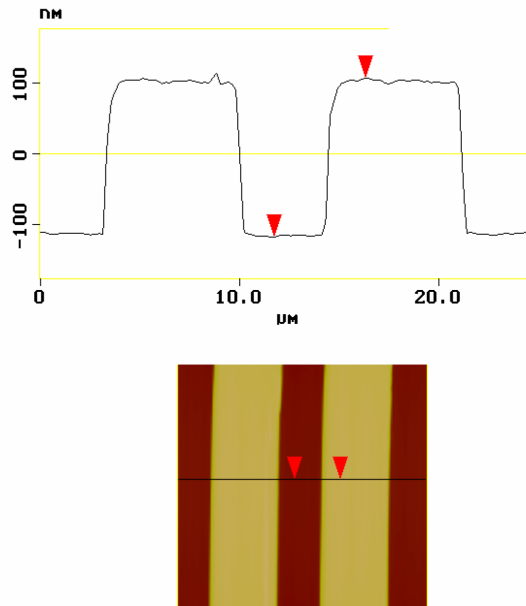

Figure 22. AFM cross-section profile of a silicon trench after dry etching in CF_4/O_2 plasma. The feature height is 200 nm.

Figure 24 is a SEM micrograph of 400-nm-diameter aluminum dots after lift-off. A comparison of the Al features and the stamp features shows no significant difference in lateral dimensions in the submicron features, proving the potential for submicron-scale stamp replication.

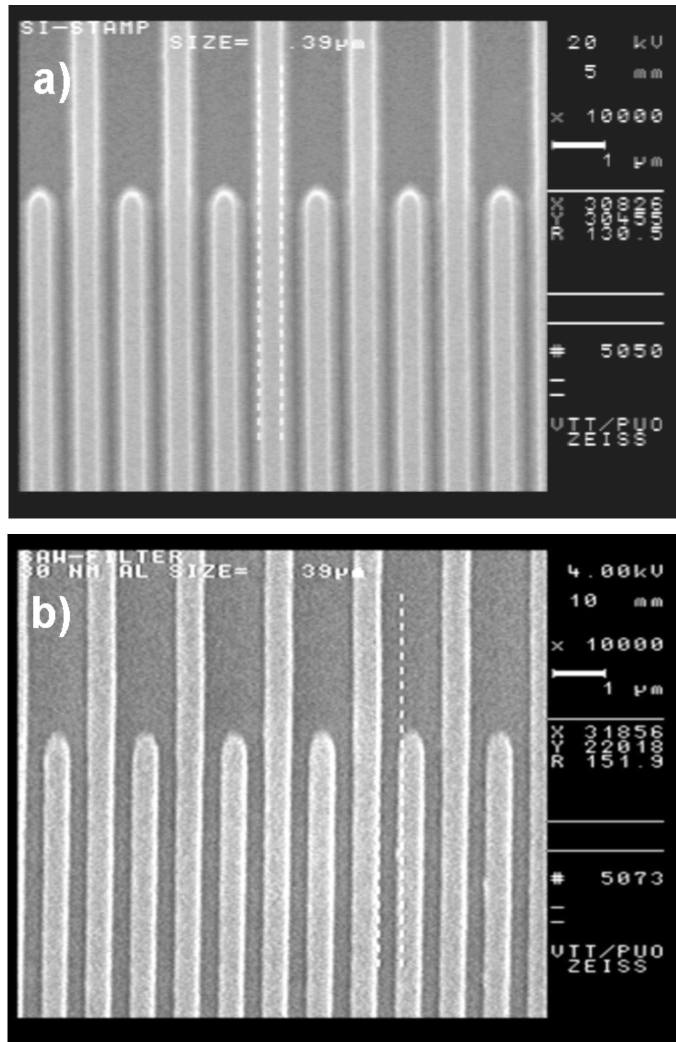

Figure 23. SEM micrograph showing the 400-nm fingers in stamp A a) and the aluminum features fabricated by imprinting and lift-off b) [I].

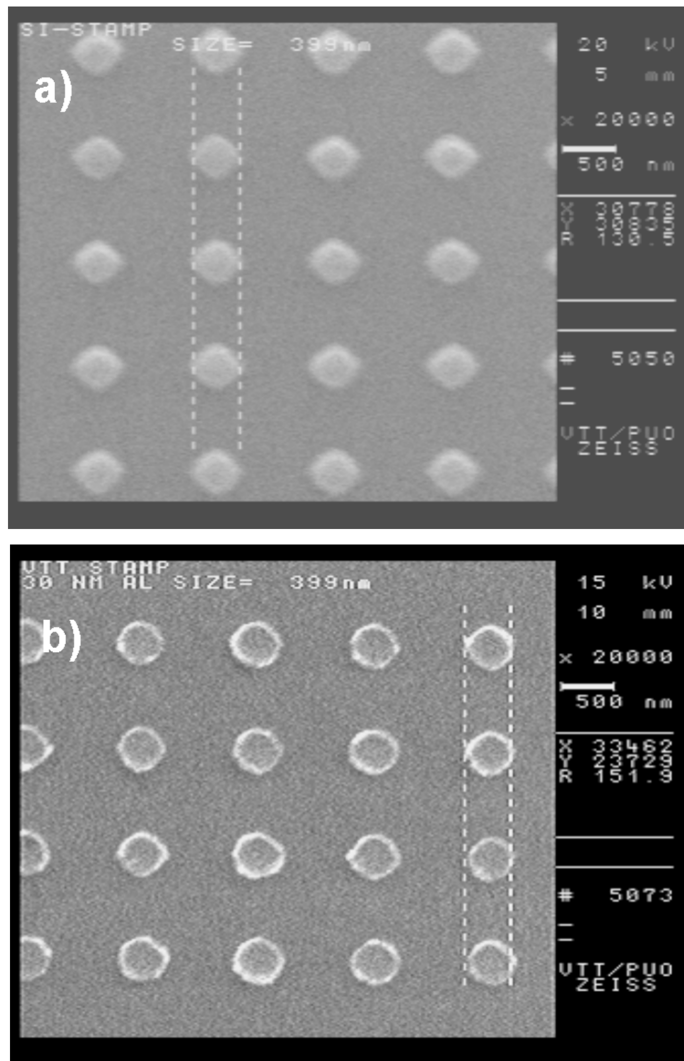

Figure 24. SEM micrograph of 400-nm dots in the silicon stamp a) and the aluminum dots fabricated by imprint lithography and lift-off b).

3.4.2 Bendable nickel stamps

Roller nanoimprint lithography (RNIL) with a cylinder mold (a thin metal film bent around a roller) was demonstrated as an alternative to flat imprint lithography in 1998 by Tan et al. [99]. The continuous roll-to-roll process has been demonstrated as a potential mass-fabrication tool for patterning devices on plastic substrate. The plastic tape is fed from a reel to an imprinting unit. The im-

printing unit consists of a thin patterned nickel film wrapped on a cylinder and a backing roll [100]. In our experimental work, roll-to-roll stamps have typically been fabricated using the electroplating process by depositing metal onto resist-coated silicon substrate. The fabrication of micron-scale features was done by patterning a light-sensitive resist by optical lithography. Figure 25 shows a nickel plate fabricated by optical lithography and a resolution mask with micron-scale test structures. The plate is cut into a rectangular shape to be fitted onto a 60-mm-wide printing roll. If stamps are wrapped over both of the rolls, the system can be used for double-sided imprinting by using a nickel stamp on both of the rolls (Figure 26). The Schematic of the construction is shown in Figure 27.

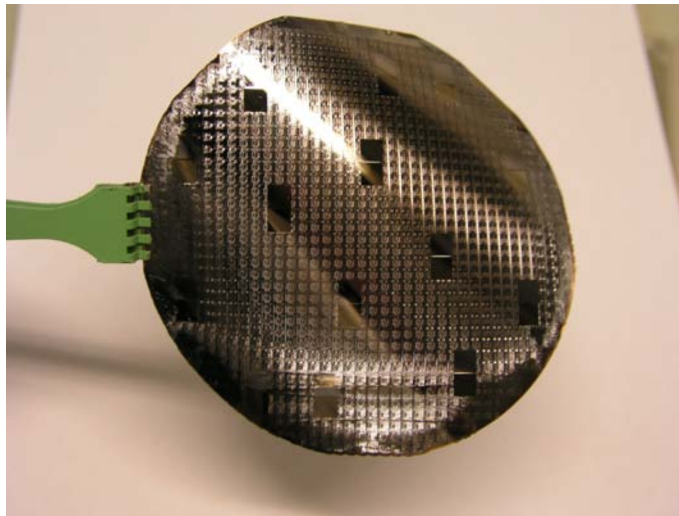

Figure 25. Nickel stamp fabricated by UV lithography using a resolution mask with micron-scale features.

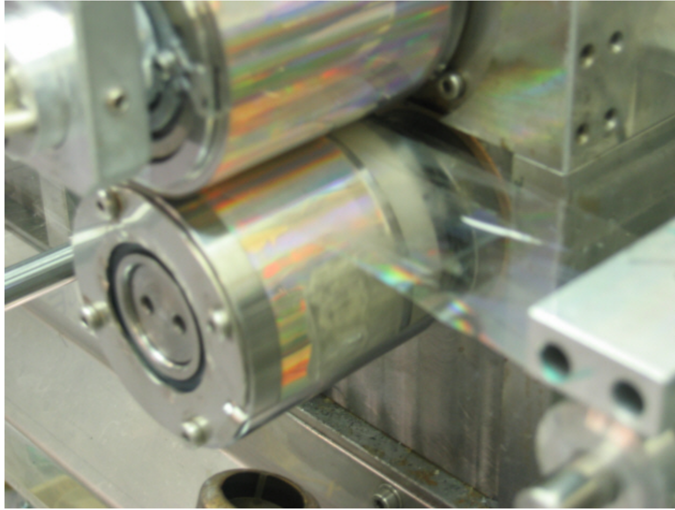

Figure 26. Printing rolls in a double simultaneous process in which nickel shims are wrapped around both rolls [IV].

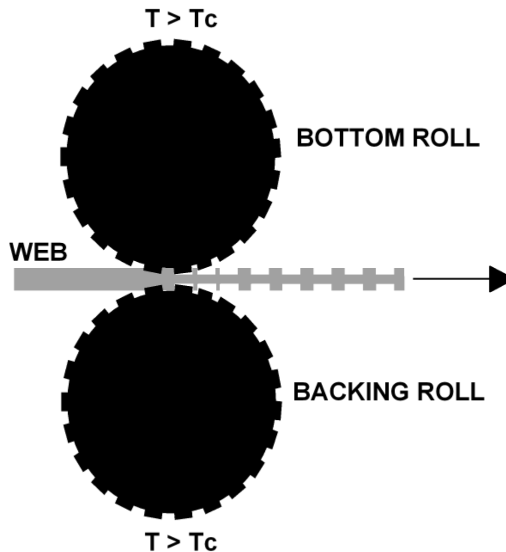

Figure 27. Schematic of the double-sided roll-to-roll imprinting system with two nickel stamps [IV].

The bendable metal stamps used in roll imprinting can be fabricated by machining metal film (laser ablation) or using a lithographic method (UV or e-beam)

and electroplating. As a mass fabrication tool, roll-to-roll imprinting requires stamps with large patterned areas. E-beam lithography lacks the high throughput and speed needed to pattern large areas effectively however. The solution introduced here is to fabricate a small stamp by EBL and use sequential imprinting to copy the structures on a large scale.

In the fabrication process, a silicon stamp is prepared using electron beam lithography and dry etching. In an example process, a silicon wafer with a thermal oxide layer is used as a starting material. The wafer is spin-coated with a negative e-beam resist, which is patterned with submicron features. The resist patterns are transferred onto the oxide layer by dry etching in CF_4/CHF_3/He plasma. In the next phase, the patterned oxide is used as a hard mask in the dry etching step in the Cl_2/He plasma to transfer the features onto silicon. The silicon wafer is then diced into small stamps.

The small stamp, in turn, is used to pattern a polymer substrate, which is used as a mold in the electroplating process. The patterned polymer mold is sputter-coated by the TiW/Cu layer, which serves as a seed metal layer. This metal layer provides electrical contact for nickel deposition in the electroplating bath. The schematic of the process is presented in Figure 28. The resist mold is lost during dissolving and can be used only once. The benefit is easy separation of the mold, and the fabrication of the resist mold is quite straightforward and relatively fast.

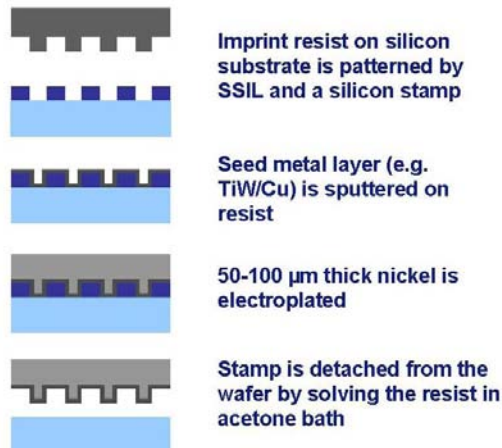

Figure 28. Schematic of the nickel stamp fabrication process by SSIL and electroplating.

Adhesion between the polymer and the metal film is poor. In order to obtain a smooth and mechanically stable field metal for Ni plating, the intrinsic stresses of the films must be minimized. The stresses in the field metal stack are mainly caused by the TiW layer. Stresses transform from compressive to tensile as a function of the sputtering pressure. The processing pressure has to be chosen in such a way that the stresses are minimized and visible cracks do not appear on the film after sputtering.

In our process, the electroplating of the nickel was carried out in a custom-cup-type plater using a Barret SN Nickel (Allied-Kelite) electrolyte bath. A pulsed power source with a current density of 67 Am^{-2} gave a deposition rate of about 8 µm/h.

Figure 29 depicts a SEM micrograph of the 100-nm-wide feature on the silicon stamp. The corresponding replicated nickel feature is shown in Figure 30. A comparison of SEM images shows that the features are preserved during replication. Figure 31 depicts the AFM image of a 180-nm-high and 100-nm-wide ridge on the nickel stamp.

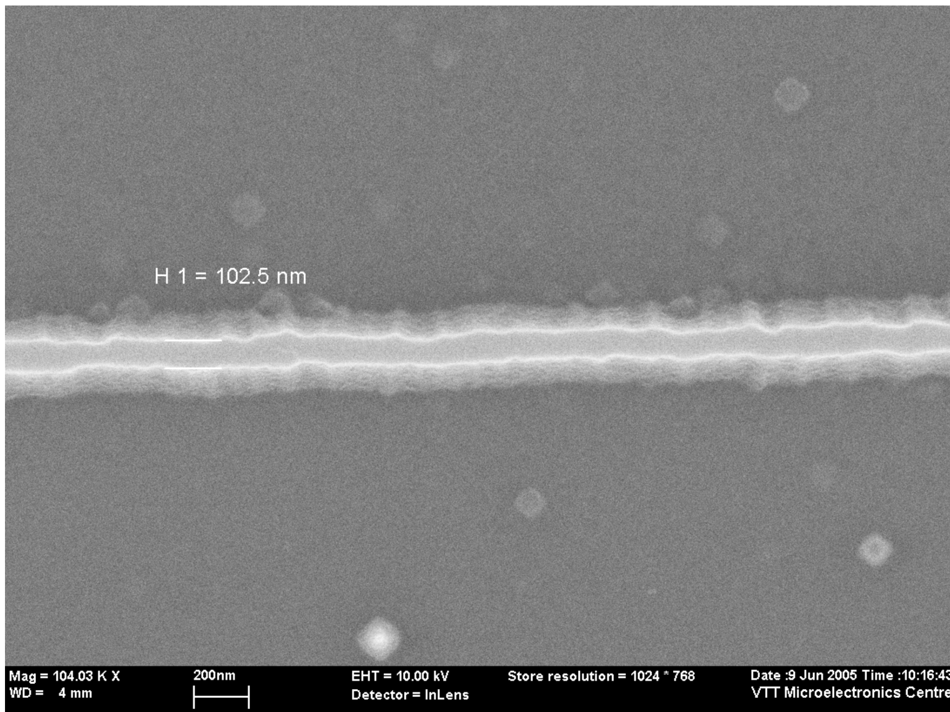

Figure 29. SEM micrograph of an e-beam patterned 100-nm-wide ridge in the silicon master after dry etching in Cl_2/He plasma [III].

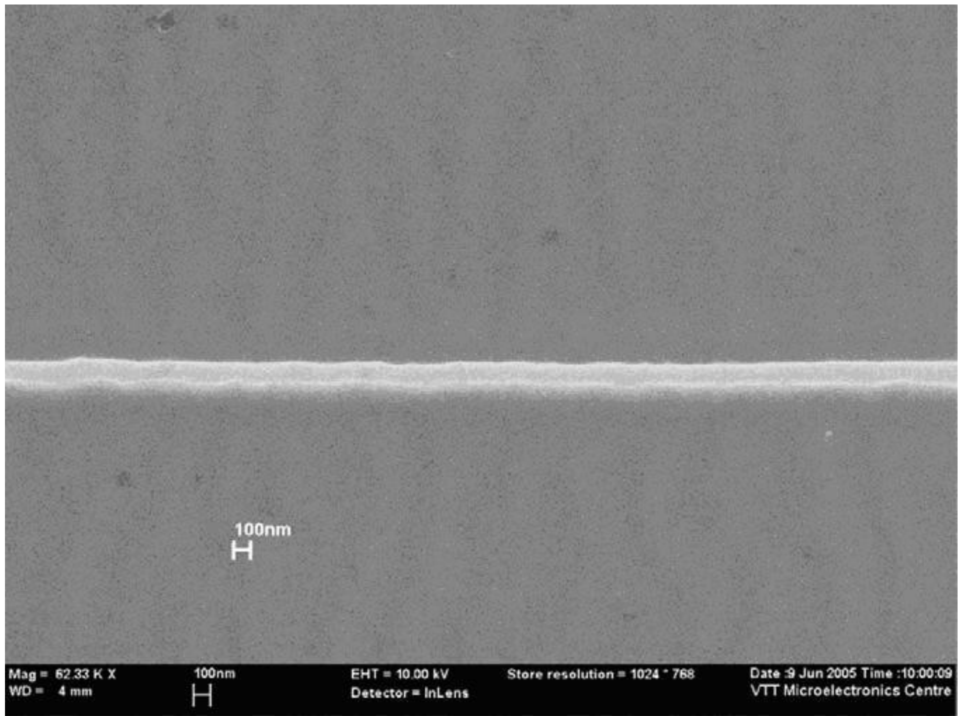

Figure 30. SEM micrograph of a 100-nm-wide and 180-nm-high ridge in the nickel stamp [III].

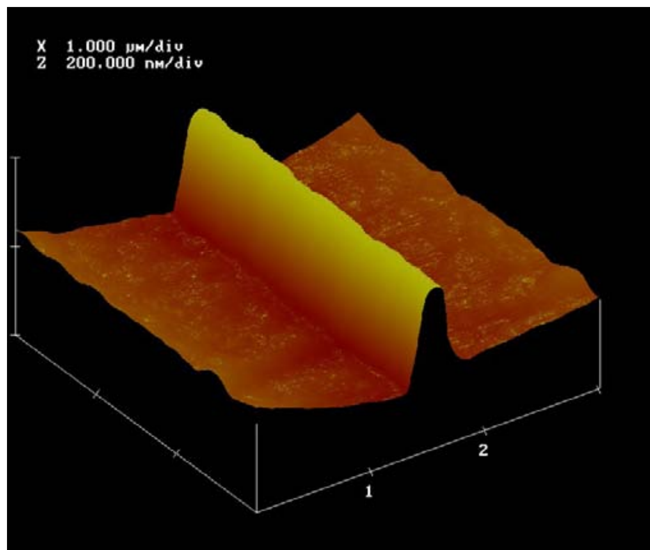

Figure 31. AFM image of a 180-nm-high ridge on the nickel stamp.

The AFM-measured surface roughness of the nickel stamp was about 8 nm. The value is more than 20 times higher than in the imprinted mr-I 7030 resist surface before metal deposition and nickel plating. The electroplating process is assumed to introduce stress into the metal film. This can be seen as increased roughness of the surface. Apart from roughness, no cracks or other visible errors were detected in the metal film.

The test runs of the stamp were made by printing onto cellulose acetate film using a custom-made laboratory scale roll-to-roll machine. The 100-nm patterns on the nickel stamp were successfully replicated onto cellulose acetate film [101].

3.4.3 UV-NIL stamps

Mold-assisted nanolithography [102], or UV-Nanoimprint Lithography (UV-NIL) [103, 104, 105, 106], has been developed in parallel with thermal NIL since 1996. Prior to this, photopolymerization had already been used in several areas of the electronics industry for the production of, for example, optical waveguides and lenses. In this method, the surface topography of the wafer-scale mold is replicated onto spin-coated, low-viscosity photo-curable polymers. Another approach is multilayer Step and Flash Imprint Lithography (S-FIL) [107, 108] in which a low-viscosity polymer is deposited onto a transfer layer on a substrate by dispensing. The cavities of the stamp are filled with capillary action. The polymer is hardened by UV radiation through the stamp. After separation, a solid replica of the mold is left on the substrate.

Like thermal SSIL, the UV Step and Stamp Imprint Lithography (UV-SSIL) uses a small stamp to pattern large areas sequentially. The small size of the stamp enables high pressures to be inserted into the structured areas. The pressure helps to minimize the residual layer in the compressed areas. The waviness or bending of the stamp or substrate also becomes less critical when reducing the size of the stamp, and the surfaces can be made flat locally. The UV-SSIL process is shown schematically in Figure 32.

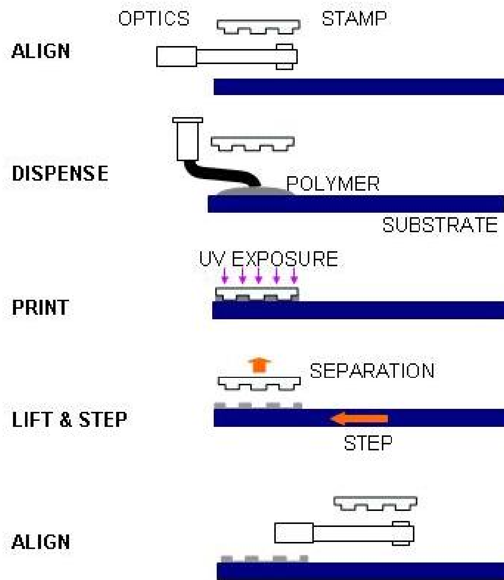

Figure 32. Principle of the UV-SSIL process. The stamp is first aligned with the substrate. The resist is dispensed to the substrate and the stamp is pressed against it. The resist is exposed through the stamp. The stamp is separated and the cycle repeated in a new location [V].

The resolution achieved in UV-NIL is better than 10 nm using a rigid quartz mold and about 50 nm using a soft PDMS mold [109]. The challenge is in patterning large areas with a highly homogenous residual layer thickness while maintaining both high resolution and alignment accuracy [110]. The property of the material is a key factor in reducing the residual layer. The thickness of the residual layer has shown to increase with the square root of the viscosity [111]. In order to reach residual layer thicknesses below 100 nm, low-viscosity materials [112] should be used.

In the UV-imprint lithography, the typical stamp material was quartz. Submicron features can be patterned by electron-beam lithography and dry etching. The stamp fabrication process corresponds to conventional phase-shift reticle processing [15]. In the standard process, a fused silica reticle is coated with a chromium layer that is a spin-coated electron beam resist. The resist is patterned by a direct-write e-beam system. After developing the resist, the chromium is etched with a Cl-based RIE through the openings. The resist is removed and silica substrate is patterned by a fluorine-based RIE and chromium mask. S-FIL

has been used to fabricate wafer-scale fused silica UV-molds using a small reticle [113] and flexible polymer molds [114]. Other fabrication methods using HSQ [115] and the Ormostamp [116] that require no RIE etching have been reported. The fabrication process, based on conventional photomask fabrication, confronts critical dimension (CD) losses during etching through the Cr layer [117]. This has motivated the search for alternatives to stamp fabrication.

The motivation for the experimental work was to develop a simple method to fabricate UV-NIL stamps with antiadhesion properties using fluorinated polymer film on top of a quartz support. The patterning was done using thermal SSIL and a silicon master. This method does not require any subsequent process steps, such as dry etching. The number of masters is not limited and a number of masters can be combined to pattern large areas. Thus, submicron-scale features and micron-scale features can be used with no need for the mix and match approach.

The fabrication of the stamp was carried out in two steps. A silicon master was prepared in the first step and used for thermal imprinting in the second step. The silicon master was patterned by UV or electron beam lithography and dry etching. The silicon master with submicron-scale features was fabricated by electron beam lithography. Correspondingly, the silicon masters with micron-scale features were defined by UV lithography. The features of the silicon master were transferred onto a polymer template by thermal imprinting (Figure 33).

Two different silicon masters were used to pattern a polymer stamp. In the first one, the features consisted of 50-nm-wide lines with a 600-nm pitch. The patterned area was 1 mm x 1 mm and the total size 3 mm x 3 mm. In the second master, the features consisted of 350-nm pillars with a 1.2-µm pitch. The stamp size was 3 mm x 3 mm patterns covering the whole area. For the fastening to the imprint machine, the silicon master is attached to a 50 mm x 50 mm SiC-support. The attachment is done using thermally conductive silicone adhesive.

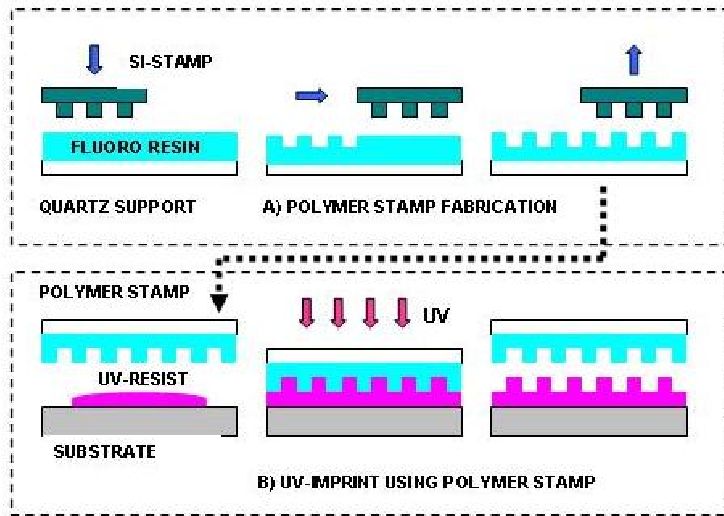

Figure 33. Schematic of the fabrication steps of a polymer stamp. A polymer template on top of the quartz plate is patterned by thermal SSIL. a). The patterned template is used as a stamp for UV imprinting b) [VI].

In the beginning of the cycle, the silicon master is aligned with the polymer template. It is then heated to 140 °C and pressed into a polymer using a pressure of 14 MPa. The pressure is maintained until the polymer flow into the cavities is complete. The temperature is reduced to 60 °C before separation. These steps were repeated until the set was completed. The master was changed for another after eight imprints, and patterning was continued with a further eight imprints.

The patterned polymer stamp was used for UV imprinting. In the process, the stamp was first aligned with the substrate. Next, a syringe-type dispenser was used to deposit the UV-curable resist UVCur06 (from microresist GmBH) onto the substrate. The material is an acrylate-based polymer with a photoinitiator. The stamp size area was dispensed by applying a matrix of the droplet (pitch 500 µm). The volume of a single droplet was about 20 nanoliters. Next, the stamp was pressed into the resist and kept in contact for 20 seconds before starting the 7 seconds curing step. The UV irradiation was realized through the stamp by an LED array (power density 120 mW/cm^2). After curing, the stamp was demolded. The substrate stage was stepped forward and the cycle was repeated at the next site on the substrate.

The patterns of the polymer stamp consisted of two by four and two by four matrices as a combination of two silicon masters. One stamp consisted of 50-nm

lines and the other of 350-nm dots. The original silicon master is shown in Figure 34, the SSIL-patterned polymer stamp in Figure 35, and the UV-imprinted replica in Figure 36. The diameter and height of the features of the silicon master and UV-cured replica were measured by AFM. The height of the replicated pillars in the UV-cured resist is 128 nm while the depth of the holes in the polymer stamp is about 132 nm. The shrinkage for mr-UVCur06 is 3–6%, so the difference is probably due to shrinkage of the polymer during cross-linking. The surface roughness of the silicon master, polymer stamp, and UV-cured resist was compared by the AFM measurement. The roughness values were 0.36 nm for the silicon master, 1 nm for the polymer stamp, and 0.93 nm for the cured UV resist. The measured surface roughness of the polymer stamp before thermal imprinting was 0.3 nm. The roughness was increased during thermal imprinting when the polymer was in contact with the silicon master.

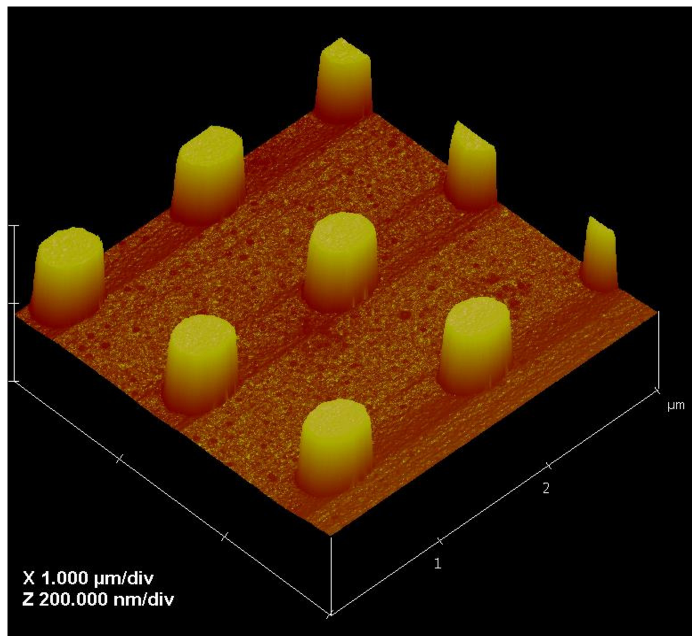

Figure 34. AFM image of a silicon stamp with 350-nm-diameter pillars. The height of the pillars is 132 nm [VI].

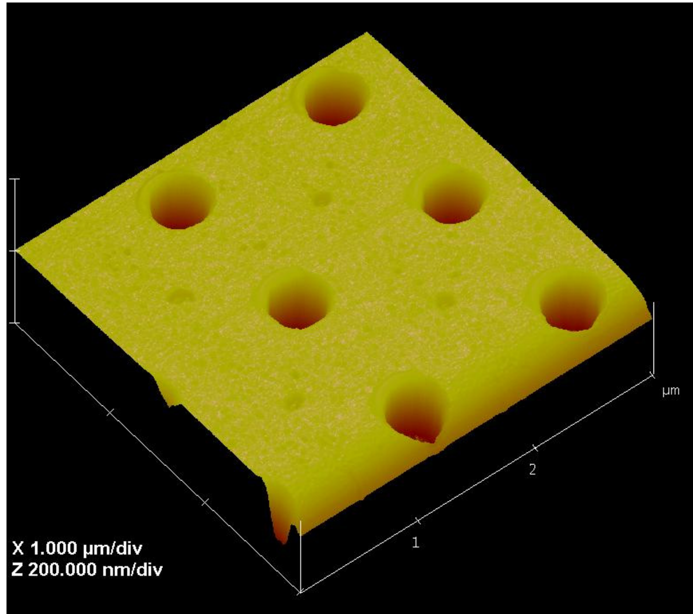

Figure 35. AFM image of 350-nm holes imprinted onto the polymer stamp. The depth of the features is 130 nm [VI].

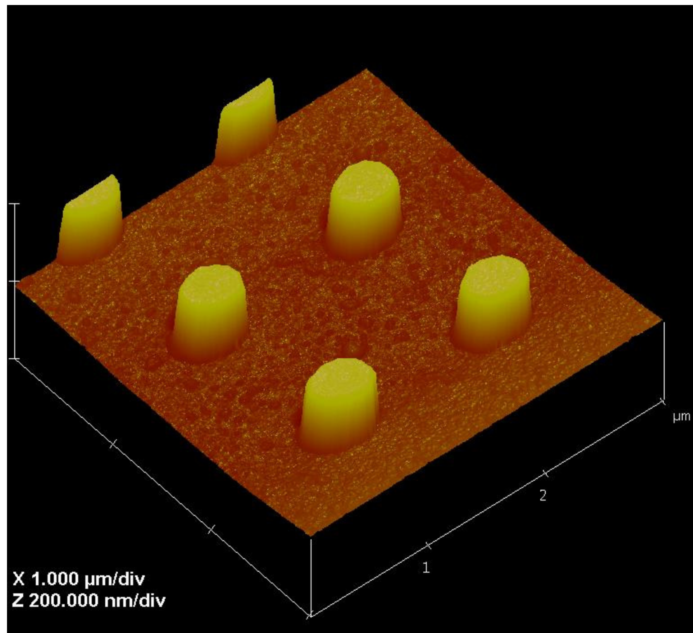

Figure 36. AFM image of 350-nm features replicated onto a UV-curable resist. The height of the pillars is 128 nm [VI].

Figure 37 depicts the 50-nm features in a cured mr-UVCur06 resist. The AFM image shows that the features of the silicon master were replicated without distortion and no resist to stamp sticking was observed during the mold release. The features in the grating are uniform and match the polymer stamp. The pattern transfer in the boundary region did not differ from the overall quality due to the gap between imprints.

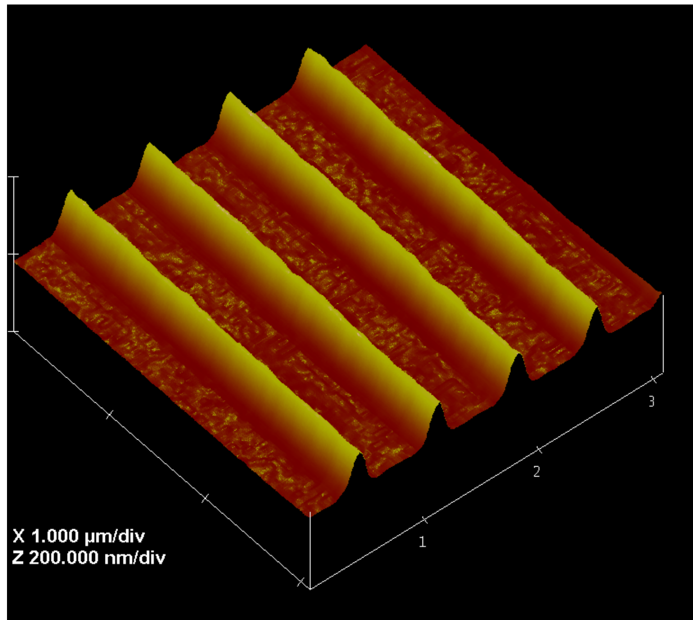

Figure 37. AFM image of 50-nm ridges in the UVcur06 resist. The patterning was done using a polymer stamp fabricated by SSIL [VI].

The fluorinated polymer of the stamp provided good mold release with an mr-UVCur06 resist. The UV-irradiant time was at the same level as when using a normal quartz stamp. The measured transmittance of the polymer stamp was 95% at the 375-nm wavelength used for UV exposure.

No sticking problems were observed in either the micron- or submicron-scale features. The fluorinated material of the stamp evidently provides good mold release with the UV resist. The UV-irradiation time was of about the same magnitude as using a normal quartz stamp. This is due to the high UV transparency of the material. The high chemical durability of the resin enables stamp cleaning with isopropyl alcohol. These attributes make the fluorinated polymer template a suitable material for the fabrication of polymer UV stamps.

4. Summary and discussion

The motivation for this work was to develop a stamp fabrication method using thermal step and stamp imprint lithography. The experimental work was initiated using a Karl Suss Flip Chip Bonder FC150. The machine was applied to imprint lithography with no hardware modifications, as the flexibility of the software allowed for the imprint application, although the machine is designed for chip onto chip bonding. On the basis of experience collected from the FC150, a dedicated imprint machine was developed by SET S.A.S. (former Suss Microtec). The new machine, NanoimPrint Stepper NPS300, had a more reliable parallelism system with a self-flexuring imprint arm to achieve final parallelism between the stamp and the substrate. The new machine has the capability to perform automatized alignment and collimation onto a maximum of 300-mm substrate with an accuracy of a quarter of a micron. The machine can be converted into UV-imprinting equipment by changing the head of the imprinting arm. With this capability, the machine can also be used to process development for small-scale pilot production.

The imprinting process was developed by optimizing the parameters temperature, pressure, and time for selected polymers. The pattern transfer onto silicon was demonstrated using both the imprinted resist and the metal mask. The metal mask was fabricated by lift-off using the imprinted resist as a mask. Large-area imprinting was realized onto 200-mm silicon substrates with features of 50-nm line width. The practical size of the silicon stamp in SSIL is limited to a few millimeters. As for larger stamps with a size of 20 mm x 20 mm, the only partial pattern replication over the stamp area was achieved due to the waviness of the substrate.

Bendable metal stamps were fabricated using imprinting to define a polymer mold and electroplating to deposit nickel onto the mold. Thus, the fabricated

metal stamp was used in a roll-to-roll imprinting process to transfer the patterns onto a CA film successfully.

The fabrication method of polymer stamps for UV-NIL was demonstrated by patterning fluorinated polymer templates by thermal SSIL using a silicon stamp. The features of the silicon stamp were replicated with good fidelity, retaining the dimensions. The tests on the polymer stamps by UV imprinting demonstrated good mold-release properties along with satisfactory pattern replication of sub-micron features, thus proving the concept useful.

In the field of thermal imprinting, the emphasis has been on the parallel processing method with large molds. In recent years, the sequential method has attracted wider interest, and a growing number of research groups have shown interest in developing sequential imprinting. The benefit of the method is flexibility, which allows patterning of each chip with a different stamp.

The parallel method has attracted a growing number of researchers due to its simplicity and low cost. In thermal step and repeat imprinting, the bottleneck is low throughput, compared with the parallel method, but the development of rapid heating and cooling of the stamp can improve the throughput significantly. Materials are also being developed all the time, and better suitability for imprint purposes can be expected in the future. Another challenge in electronic applications is multilevel capability with an overlay accuracy of tens of nanometers on wafers larger than 150 mm in diameter. Applications relying on single layer patterning, such as optical gratings, are not as demanding in overlay accuracy and can be realized sooner in mass production.

There are many applications in sight in nanoimprint lithography that require sophisticated stamp fabrication technology for optical, photonic, electrical, and biological applications. Nanoimprint lithography is suitable for patterning 3D features used in, for example, optical devices such as sawtooth diffractive grating elements or anti-reflection surfaces. There are many other applications in the field of optics, such as photonic crystals, light directional elements for extracting light from LEDs, and control deviation of light in window glass surfaces for use in natural lighting for housing. There are different sensors for nano-bio research, such as interdigitated nanoelectrodes. In electrical application, imprinting can be used for, for example, fabrication of MOSFETs and organic FETs.

References

[1] Ronse, K. Optical lithography – a historical perspective. C. R. Physique 7 (2006), pp. 844–857.

[2] Lawes, R.A. Future trends in high-resolution lithography. Appl. Surf. Sci. 154–155 (2000), pp. 519–526.

[3] Lin, B.J. Optical lithography – present and future challenges. C. R. Physique 7 (2006), pp. 858–874.

[4] Fay, B. Advanced optical lithography development from UV to EUV. Microelectron. Eng. 61–62 (2002), pp. 11–24.

[5] Kemp, K. and Wurn, S. EUV lithography. C. R. Physique 7 (2006), pp. 875–886.

[6] Peckerar, M. C. and Maldonado, J. R. X-ray Lithography – An Overview. Proc. IEEE 81 (1993), pp. 1249–1274.

[7] Iwamitsu, S., Nagao, M., Shahjada, S., Pahlovy, A., Nishimura, K., Kashihara, M., Momota, S., Nojiri, Y., Taniguchi, J., Miyamoto, I., Nakao, T., Morita, N. and Kawasegi, N. Ion beam lithography by using highly charged ion beam of Ar. Colloids and Surfaces A: Physicochem. Eng. Aspects 313–314 (2008), pp. 407–410.

[8] Vieu, C., Carcenac, F., Pepin, A., Chen, Y., Mejias, M., Lebib, A., Manin-Ferlazzo, L., Couraud, L. and Launois, H. Electron beam lithography: resolution limits and applications. Appl. Surf. Sci. 164 (2000), pp. 111–117.

[9] Chou, S. Y., Krauss, P. R. and Renstrom, P. J. Imprint of sub-25 nm via and trenches in polymers. Appl. Phys. Lett. Vol. 67 No. 21 (1995), pp. 3114–3116.

[10] Derbyshire, B. The ancient technique of imprint lithography could make a mark on next–generation wafer patterning. Semiconductor Manufacturing, July (2004), pp. 19–26.

[11] Chou, S. Y., Krauss, P. R. and Renstrom, P. J. Nanoimprint lithography. J. Vac. Sci. Vol. B14, No. 6 (1996), pp. 4129–4133.

[12] Chou, S. Y. and Kraus, P. R. Imprint Lithography with Sub-10 nm Feature Size and High Throughput. Microelectronic Eng. 35 (1997), pp. 237–240.

[13] Sotomayor Torres, C.M., Zankovych, S., Seekamp, J., Kamm, A.P., Cedeno, C. C., Hoffmann, T., Ahopelto, J., Reuther, F., Pfeiffer, K., Bleidiessel, G., Gruetzner, G., Maximov, M.V. and Heidari, B. Nanoimprint lithography: an alternative nanofabrication approach. Mater. Sci. and Eng. C23 (2003), pp. 23–31.

[14] Guo, L.J. Recent progress in nanoimprint technology and its applications. J. Phys. D: Appl. Phys. 37 (2004), pp. R123–R141.

[15] Alternative Lithography: Unleashing the potentials of Nanotechnology, edited by Sotomayor-Torres, C. M., University of Wuppertal, Kluwer Academic/Plenum Publishers, New York 2003.

[16] Becker, H. and Heim, U. Hot embossing as a method for the fabrication of polymer high aspect ratio structures. Sensors and Actuators 83 (2000), pp. 130–135.

[17] Yokoo, A., Suzuki, H. and Notomi, M. Organic Photonic Crystal Band Edge Laser Fabricated by Direct Nanoimprinting. Japanese Journal of Applied Physics 43 (2004), pp. 4009–4011.

[18] Hoon Kim, S., Lee K.-D., Kim J.-Y., Kwon M.-K. and Seong-Ju Park. Fabrication of photonic crystal structures on light emitting diodes by nanoimprint lithography. Nanotechnology 18 (2007), pp. 1–5.

[19] Kang, D.J., Bae, B.-S. and Nishi, J. Fabrication of Thermally Durable subwavelength Periodic Structures upon Inorganic Hybrid Materials by Nanoimprinting. Japanese Journal of applied Physics 46(6A) (2007), pp. 3704–3709.

[20] Yu, Z., Schablitsky, S.J. and Chou, S.Y. Nanoscale GaAs metal-semiconductor-metal photodetectors fabricated using nanoimprint lithography. Appl. Phys. Lett. 74(16) (1999), pp. 2381–2383.

[21] Baba, A., Hizukuri, M., Iwamoto, M. and Asano, T. Stamp Technology for fabrication of field emitter from organic material. J. Vac. Sci. Technol. B18(2) (2000), pp. 877–879.

[22] Guo, L., Krauss, P.R. and Chou, S.Y. Nanoscale silicon field effect transistors fabricated using imprint lithography. App. Phys. Lett. 71(13) (1997), pp. 1881–1883.

[23] Schift, H., Jaszewski, R.W., David, C. and Gobrecht, J. Nanostructuring of polymers and fabrication of interdigitated electrodes by hot embossing lithography. Microelectron. Eng. 46 (1999), pp. 121–124.

[24] Wu, W., Cui, B., Sun, X., Zhang, W., Zhuang, L. and Kong, L. Large area high density quantized magnetic disks fabricated using nanoimprinting lithography. J. Vac. Sci. Technol. B16(6), pp. 3825–3829.

[25] Krauss, P.R. and Chou, S.Y. Nano-compact disks with 400 Gbit/in2 storage density fabricated using nanoimprint lithography and read with proximal probe. Appl. Phys. Lett. 71(21) (1997), pp. 3174–3176.

[26] Chen, Y., Lebib, A., Li, S.P., Natali, M., Peyrade, D. and Cambril, E. Nanoimprint fabrication of micro–rings for magnetization reversal studies. Microelectron. Eng. 57–58 (2001), pp. 405–410.

[27] Li, M., Chen, L. and Chou, S.Y. Direct three-dimensional patterning using nanoimprint lithography. Appl. Phys. Lett. 78(21) (2001), pp. 3322–3324.

[28] Schift, H., Park, S. and Gobrecht, J. Nano-Imprint – Molding Resists for Lithography. J. Photopolym. Sci. Technol 16 No.3 (2003), pp. 435–438.

[29] Jackson, A.P., Liu, X.-L. and Paton, R. Squeeze flow characterisation of thermoplastic polymer. Composite Structures 75 (2006), pp. 179–184.

[30] Heyderman, L.J., Schift H., David C., Gobrecht, J. and Schweizer T. Flow behaviour of thin films used for hot embossing lithography. Microelectronic Eng. 54 (2000), pp. 229–245.

[31] Scheer, H.-C. and Schulz, H. A contribution to the flow behaviour of thin polymer films during hot embossing lithography. Microelectronic Eng. 56 (2001), pp. 311–332.

[32] Schulz, H., Wissen, M., Bogdanski, N., Scheer, H.-C., Mattes, K. and Friedrich, Ch. Impact of molecular weight of polymers and shear rate effects for nanoimprint lithography. Microelectron. Eng. 83 (2006), pp. 259–280.

[33] Liang, J.-Z. Characteristics of melt shear viscosity during extrusion of polymers. Polymer Testing 21 (2002), pp. 307–311.

[34] Lazzarino, F., Gourgon, C., Schiavone, P. and Perret, C. Mold deformation in nanoimprint lithography. J. Vac. Sci. Technol. B22(6) (2004), pp. 3318–3322.

[35] Merino, S., Retolaza, A., Schift, H., and Trabadelo, V. Stamp deformation and its influence on residual layer homogeneity in thermal nanoimprint lithography. Microelectron. Eng. 85 (2008), pp. 877–880.

[36] Sirotkin, V., Svintsov, A., Schift, H., and Zaitsev S. Coarse-grain method for modelling of stamp and substrate deformation in nanoimprint. Microelectron. Eng. 84 (2007), pp. 868–871.

[37] Vinogradov, G.V. and Malkin, A. Ya. Rheology of Polymers, Mir Publisher, Moscow (1980).

[38] Gourgon, C., Perret, C., Micouin, G., Lazzarino, F., Tortal, J. H. and Joubert, O. Influence of pattern density in nanoimprint lithography. J. Vac. Sci. Technol. B21(1) (2003), pp. 98–105.

[39] Scheer, H.-C., Bogdanski, N., Wissen, M. and Möllenbeck, S. Imprintability of polymer for thermal nanoimprint. Microelectron. Eng. 85 (2008), pp. 890–896.

[40] Schulz, H., Wissen, M. and Scheer, H.-C. Local mass transport and its effect on global pattern replication during hot embossing. Microelectronic Eng. 67–68 (2003), pp. 657–663.

[41] Hirai, Y., Onishi, Y., Tanabe, T., Shibata, M., Iwasaki, T. and Iriye, Y. Pressure and resist thickness dependency of resist time evolutions profiles in nanoimprint lithography. Microelectron. Eng. 85 (2008), pp. 842–845.

[42] Hirai, Y., Konishi, T., Yoshikawa, T. and Yoshida, S. Simulation and experimental study of polymer deformation in nanoimprint lithography. J. Vac. Sci. Technol. B 22(6) (2004), pp. 3288–3293.

[43] Kehagias, N., Reboud, V., Sotomayor-Torres, C. M., Sirotkin, V., Svintsov, A. and Zaitsev, S. Residual layer thickness in nanoimprint: Experiments and coarse-grain simulation. Microelectron. Eng. 85 (2008), pp. 846–849.

[44] Young, W.-B. Analysis of the nanoimprint lithography with viscous flow model. Microelectron. Eng. 77 (2005), pp. 405–411.

[45] Sirotkin, V., Svintsov, A., Zaitsev, S. and Schift, H. Viscous flow simulation in nanoimprint using coarse-grain method. Microelectron. Eng. 83 (2006), pp. 880–883.

[46] Rowland, H.D., Sun, A. C., Schunk, P.R. and King, W.P. Impact of polymer film thickness and cavity size on polymer flow during embossing: toward process design rules for nanoimprinting lithography. J. Micromech. Microeng. 15 (2005), pp. 2414–2425.

[47] Scheer H.-C., Bogdanski N., Wissen M., Konishi T., Hirai Y. Profile evolution during thermal nanoimprint. Microelectronic Eng. 83 (2006), pp. 843–846.

[48] Bogdanski, N., Wissen, M., Möllenbeck, S., and Scheer, H.-C. Thermal Imprint with negligibly low residual layer. J. Vac. Sci. B24(6) (2006), pp. 2998–3001.

[49] Bogdanski, N., Wissen, M., Ziegler, A. and Scheer, H.-C. Temperature-reduced nanoimprint lithography for thin and uniform residual layers. Microelectron. Eng. 78–79 (2005), pp. 598–604.

[50] Bogdanski, N., Wissen, M., Möllenbeck, S. and Scheer, H.-C. Structure size dependent recovery of thin polystyrene layers in thermal imprint lithography. Microelectron. Eng. 84 (2007), pp. 860–863.

[51] Chen, Y., Macintyre, D.S. and Thoms, S. A non–destructive method for the removal residual resist in imprinted patterns. Microelectronic Eng. 67–68 (2003), pp. 245–251.

[52] Lebib, A., Chen, Y., Carcenac, F., Cambril, E., Mann, L., Couraud, L. and Launois, H. Tri-layer systems for nanoimprint lithography with an improved process latitude. Microelectronic Eng. 53 (2000), pp. 175–178.

[53] Lebib, Y., Chen, Y., Cambril, E., Youinou, P., Studer, V., Natali, M., Pepin, A., Janssen, H.M. and Sijbesma, R.P. Room-temperature and low-pressure nanoimprint lithography. Microelectron. Eng. 61–62 (2002), pp. 371–377.

[54] Carlberg, P., Grazyck, M., Sarwe, E.-L., Maximov, I., Beck, M. and Montelius, L. Lift-off process for nanoimprint lithography. Microelectron. Eng. 67–68 (2003), pp. 203–207.

[55] Sun, X., Zhuang, L., Zhang, W. and Chou, S.Y. Multilayer resist methods for nanoimprint lithography on nonflat surfaces. J. Vac. Sci. Technol. B16(6) (1998), pp. 3922–3925.

[56] Jaszewski, R.W., Schift, H., Gobrecht, J. and Smith, P. Hot embossing in polymers as a direct way to pattern resist. Microelectronic Eng. 41/42 (1998), pp. 575–578.

[57] Gottschalch, F., Hoffmann, T., Sotomayor Torres, C.M., Schulz, H. and Scheer, H.-C. Polymer issues in nanoimprinting technique. Solid-State Electronics 43 (1999), pp. 1079–1083.

[58] Scheer, H.C., Schulz, H., Hoffmann, T. and Sotomayor Torres, C.M. Problem of the nanoimprinting technique for nanometer scale pattern definition. J. Vac. Sci. B16(6) (1998), pp. 3917–3921.

[59] Pfeiffer, K., Bleidiessel, G., Grueztner, G., Schulz, H., Hoffmann, T., Scheer, H.-C., Sotomayor Torres, C. M. and Ahopelto, J. Suitability of new polymer materials with adjustable glass temperature for nanoimprinting. Micro- and Nanoengineering Conference, MNE ’98, Leuven.

[60] Gourgon, C., Perret, C. and Micouin, G. Electron beam photoresist for nanoimprint lithography. Microelectron. Eng. 61–62 (2002), pp. 385–392.

[61] Gaboriau, F., Peignon, M.C., Barreau, A., Turban, G. and Cardinaud, Ch. High density fluorocarbon plasma etching for new resists suitable for nano-imprint lithography. Microelectronic Eng. 53 (2000), pp. 501–505.

[62] Pfeiffer, K., Finck, M., Bleidiessel, G., Grueztner, G., Schulz, H., Scheer, H.-C., Hoffmann, T., Sotomayor Torres, C.M., Gaboriau, F., and Cardinaud, Ch. Novel linear and crosslinking polymers for nanoimprinting with high etch resistance. Microelectronic Eng. 53 (2000), pp. 411–414.

[63] Schulz, H., Scheer, H.-C., Hoffmann, T., Sotomayor Torres, C. M., Pfeiffer, K., Bleidiessel, G., Grueztner, G., Cardinaud, Ch., Gaboriau, F., Peignon, M.-C., Ahopelto, J. and Heidari, B. New polymer materials for nanoimprinting. J. Vac. Sci. Technol. B18(4) (2000), pp. 1861–1865.

[64] Casey, B.G., Monaghan, W. and Wilkinson, C.D.W. Embossing of Nanoscale Features and Environments. Microelectronic Eng. 35 (1997), pp. 393–396.

[65] Dreuth, H. and Heiden, C. Thermoplastic structuring of thin polymer films. Sensors and Actuators 78 (1999), pp. 198–204.

[66] Yokoo, A., Nakao, M., Yoshikawa, H., Masuda, H. and Tamamura, T. 63-nm-Pitch Pit Pattern Fabricated on Polycarbonate surface by Direct Nanoimprinting. Jpn. J. Appl. Phys. 38 (1999), pp. 7268–7271.

[67] Hirai, Y., Kanakugi, K., Yamaguchi, T., Yao, K., Kitakawa, S., and Tanaka, Y. Fine pattern fabrication on glass surface by imprint lithography. Microelectron. Eng. 67–68 (2003), pp. 237–244.

[68] Chou, S.Y., Keimel, C. and Gu, J. Ultrafast and direct imprint of nanostructures in silicon. Nature 417 (2002), pp. 835–837.

[69] Kawata, H., Yasuda, M. and Hirai, Y. Fabrication of Si mold with smooth side wall by new plasma etching process. Microelectron. Eng. 84 (2007), pp. 1140–1143.

[70] Maximov, I., Sarwe, E.-L., Beck, M., Deppert, K., Graczyk, M., Magnusson, M.H. and Montelius L. Fabrication of Si-based nanoimprint stamps with sub-20 nm features. Microelectron. Eng. 61–62 (2002), pp. 449–454.

[71] Zhao, Y., Berenschot, E., de Boer, M., Jansen, H., Tas, N., Huskens, J. and Elwenspoek, M. Fabrication of a silicon oxide stamp by edge lithography reinforced with silicon nitride for nanoimprint lithography. J. Micromech. Eng. 18 (2008), pp. 1–6.

[72] Alkaisi, M.M., Blaikie, R.J. and McNab, S.J. Low temperature nanoimprint lithography using silicon nitride molds. Microelectron. Eng. 57–58 (2001), pp. 367–373.

[73] Youn, S.-W., Okuyama, C., Takahashi, M. and Maeda, R. A study on fabrication of silicon mold for polymer hot-embossing using focused ion beam milling. Journal of Material Processing Technology 201 (2008), pp. 548–553.

[74] Kim, C.S., Park, J., Chu, W. S., Jang, D.Y., Kim, S.D. and Ahn, S.H. Fabrication of silicon micro-mould for polymer replication using focused ion beam. Microelectron. Eng. 86 (2009), pp. 556–560.

[75] Byeon, K.-J., Yang, K.-Y. and Lee, H. Thermal imprint lithography using submicron sized nickel template coated with thin SiO2 layer. Microelectron. Eng. 84 (2007), pp. 1003–1006.

[76] Hong S.-H., Lee J.-H. and Lee, H. Fabrication of 50 nm patterned nickel stamp with hot embossing and electroforming process. Microelectron. Eng. 84 (2007), pp. 977–979.

[77] Pfeiffer, K., Fink, M., Ahrens, G., Gruetzner, G., Reuther, F., Seekamp, J., Zankovych, S., Sotomayor Torres, C. M., Maximov, I., Beck, M., Graczyk, M., Montelius, L., Schulz, H., Scheer, H.-C. and Steingrueber, F. Polymer stamps for nanoimprinting. Microelectron. Eng. 61–62 (2002), pp. 393–398.

[78] Schulz, H., Lyebyedev, D., Scheer, H.-C., Pfeiffer, K., Bleidiessel, G., Gruztner, G. and Ahopelto, J. Master replication into thermosetting polymer for nanoimprinting. J. Vac. Sci. Technol. B18(6) (2000), pp. 3582–3585.

[79] Roos, M., Schulz, H., Bendfeldt, L., Fink, M., Pfeiffer, K. and Scheer, H.-C. First and second generation purely thermoset stamps for hot embossing. Microelectron. Eng. 61–62 (2002), pp. 399–405.

[80] Gadegaard, N. and McCloy, D. Direct stamp fabrication for NIL and hot embossing using HSQ. Microelectron. Eng. 84 (2007), pp. 2785–2789.

[81] Koerner, T., Brown, L., Xie, R. and Oleschuk, R.D. Epoxy resins as stamps for hot embossing of microstructures and microfluidic channels. Sensors and Actuators B 107 (2005), pp. 632–639.

[82] Tan, L., Kong, Y.P., Bao, L.-R., Huang, X.D., Guo, L.J., Pang, S.W. and Yee, A.F. Imprinting polymer film on patterned substrates. J. Vac. Sci. Technol. B21(6) (2003), pp. 2742–2748.

[83] Jo, S.-B., Lee, M.-W., Park, S.G., Suh, J.-K., and O, B.-h. Fabrication and surface treatment of silicon mold for polymer microarray. Surface & Coating Technology 188–189 (2004), pp. 452–458.

[84] Jaszewski, R.W., Schift, H., Gröning, P. and Margaritondo, G. Properties of thin anti-adhesive films used for the replication of microstructures in polymers. Microelectronic Eng. 35 (1997), pp. 381–384.

[85] Jaszewski, R.W., Schift, H., Schnyder, B., Schneuwly, A. and Gröning, P. The deposition of anti-adhesive ultra-thin Teflon-like films and their interaction with polymer during hot embossing. Appl. Surface Sci. 143 (1999), pp. 301–308.

[86] Beck, M., Graczyk, M., Maximov, I., Sarwe, E.-L., Ling, T.G.I, Keil, M. and Montelius, L. Improving stamps for 10 nm level wafer scale nanoimprint lithography. Microelectron. Eng. 61–62 (2002), pp. 441–448.

[87] Park, S., Padeste, C., Shift, H. and Gobrecht, J. Nanostructuring of anti-adhesive layer by hot embossing lithography. Microelectron. Eng. 67–68 (2003), pp. 252–258.

[88] Schift, H., Saxer, S., Park, S., Padeste, C., Pieles, U. and Gobrecht, J. Controlled co-evaporation of silanes for nanoimprint stamps. Nanotechnology 16 (2005), pp. 171–175.

[89] Sun, H., Liu, J., Gu, P. and Chen, D. Anti–sticking treatment for a nanoimprint stamp. Applied Surface Science 254 (2008), pp. 2955–2959.

[90] Tallal, J., Gordon, M., Berton, K., Charkey, A. L. and Peyrade, D. AFM characterization of anti-sticking layers used in nanoimprint. Microelectron. Eng. 83 (2006), pp. 851–854.

[91] http://www.setsas.fr

[92] http://www.dowcorning.com

[93] Heidari, B., Maximov, I., Sarwe, E.-L. and Montelius, L. Large Scale Nanolithography using Nanoimprint Lithography. J. Vac. Sci. Technol. B17 (1999), pp. 2961–2964.

[94] Lebib, A., Bourneix, J., Carcenac, F., Cambril, E., Couraud, L. and Launois, H. Nanoimprint lithography for large area pattern replication. Microelectronic Eng. 46 (1999), pp. 319–322.

[95] Khang, D.-Y. and Lee, H.H. Wafer-scale sub-micron lithography. Applied Physics Letters vol. 75. No. 17 (1999), pp. 2599–2601.

[96] Schift, H., David, C., Gabriel, M., Gobrecht, J., Heyderman, L.J., Kaiser, W., Köppel, S. and Scandella, L. Nanoreplication in polymers using hot embossing and injection molding. Microelectronic Eng. 53 (2000), pp. 171–174.

[97] http://www.mrt.de

[98] Reuther, F. Advanced Polymers and Resists – A Key to the Development of Nanoimprint Lithography. J. Photopolym. Sci. Technol. 18(4) (2005), pp. 525–530.

[99] Tan, H., Gilbertson, A. and Chou, S.Y. Roller nanoimprint lithography. J. Vac. Sci. Technol. B16(6) (1998), pp. 3926–3928.

[100] Mäkelä, T. Towards printed electronics devices. Ph.D. Thesis, VTT Publications 674 (2008). 61 p. + app. 28 p.
http://www.vtt.fi/inf/pdf/publications/2008/P674.pdf

[101] Mäkelä, T. and Ahopelto, J. Advanced Technologies and Applications of Nanoimprint. Edited by Y. Hirai. Frontier Publishing Co. Tokyo (2008), pp. 61–66.

[102] Haisma, J., Verheijen, M. and van den Heuvel, K. Mold-assisted lithography: A process for reliable pattern replication. J. Vac. Sci. Technol. B14(6) (1996), pp. 4124–4128.

[103] Bender, M., Otto, M., Hadam, B., Vratzov, B., Spangenberg, B. and Kurz, H. Fabrication of Nanostructures using UV-based imprint technique. Microelectron. Eng. 53 (2000), pp. 233–236.

[104] Vratzov, B., Fuchs, A., Lemme, M., Henschel, W. and Kurz, H. Large scale UV based nanoimprint lithography. J. Vac. Sci. Technol. B 21(6) (2003), p. 2760.

[105] Otto, M., Bender, M., Hadam, B., Spangenberg, B. and Kurz, H. Characterization and application of UV-based imprint technique. Microelectron. Eng. 57–58 (2001), pp. 361–366.

[106] Plachetka, U., Bender, M., Fuchs, A., Vratsov, B., Glinsner, T., Lindner, F. and Kurz, H. Wafer scale patterning by soft UV-Nanoimprint Lithography. Microelectron. Eng. 73–74 (2004), pp. 167–171.

[107] Bailey, T., Smith, B., Choi, B.J., Colburn, M., Meissl, M., Sreenivasan, S.V., Ekerdt, J.G. and Willson, C.G. Step and flash imprint lithography: Defect analysis. J. Vac. Sci. Technol. B19(6) (2001), pp. 2806–2810.

[108] Resnick, D.J., Sreenivasan, S.V. and Wilson, C.G. Step&flash imprint lithography. Mater. Today 8(2) (2005), pp. 34–42.

[109] Bender, M., Fuchs, A., Plachetka, U. and Kurz, H. Status and prospects of UV-Nanoimprinting technology. Microelectron. Eng. 83 (2006), pp. 827–830.

[110] Fuchs, A., Bender, M., Plachetka, U., Kock, L., Koo, N., Wahlbrink, T. and Kurz, H. Lithography potentials of UV-nanoimprint. Current Apl. Phys. 8 (2008), pp. 669–674.

[111] Schmitt, H., Frey, L., Ryssel, H., Rommel, M. and Lehrer, C.K. UV nanoimprint materials: Surface energies, residual layers, and imprint quality. J. Vac. Sci. Technol. B25(3) (2007), pp. 785–790.

[112] Kawaguchi, Y., Nonaka, F. and Sanada, Y. Fluorinated materials for UV nanoimprint lithography. Microelectron. Eng. 84 (2007), pp. 973–976.

[113] Miller, M., Schmid, G., Doyle, G., Thompson, E. and Resnick, D.J. Template replication for full wafer imprint lithography. Microelectron. Eng. 84 (2007), pp. 885–890.

[114] Hong, S.-H., Hwang, J.-Y., Lee, H., Lee, H.-C. and Choi, K.-W. UV nanoimprint using flexible polymer template and substrate. Microelectron. Eng. 86 (2009), pp. 295–298.

[115] Kehagias, N., Reboud, V., De Girolamo, J., Chouiki, M., Zelsmann, M., Boussey, J. and Sotomayor Torres, C.M. Stamp replication for thermal and UV nanoimprint lithography using a UV-sensitive silsesquioxane resist. Microelectron. Eng. 86 (2009), pp. 776–778.

[116] Klukowska, A., Kolander, A., Bergmair, I., Muhlberger, M., Leichtfried, H., Reuther, F., Grutzner, G. and Schöfner, R. Novel transparent hybrid polymer working stamp for UV-imprinting. Microelectron. Eng. 86 (2009), pp. 697–699.

[117] Bailey, T.C., Resnick, D.J., Mancini, D., Nordquist, K.J., Dauksher, W.J., Ainley, E., Talin. A., Gehoski K., Baker, J.H., Choi, B. J., Johnson, S., Colburn, M., Meissl, M., Sreenivasan, S.V., Ekerdt, J. G. and Willson, C.G. Template fabrication schemes for step and flash imprint lithography. Microelectron. Eng. 61–62 (2002), pp. 461–467.

Papers I–VIII are not included in the PDF version.
Please order the printed version to get the complete publication
(http://www.vtt.fi/publications/index.jsp).

Series title, number and report code of publication

VTT Publications 758
VTT-PUBS-758

Author(s)
Tomi Haatainen

Title
Stamp fabrication by step and stamp nano-imprinting

Abstract
The nanoimprinting is a potential method for submicron scale patterning for various applications, for example, electric, photonic and optical devices. The patterns are created by mechanical deformation of imprint resist using a patterned imprinting mold called also a stamp. The bottle-neck for imprint lithography is availability of the stamps with nanometer-scale features, which are typically fabricated by electron beam lithography. Therefore, patterning of a large stamp is time consuming and expensive. Nanoimprint lithography can offer a low cost and a high through-put method to replicate these imprinting molds.

In this work, stamp replication process was developed and demonstrated for three different types of imprint molds. Replication relies on sequential patterning method called step and stamp nanoimprint lithography (SSIL). In this method a small master mold is used to pattern large areas sequentially. The fabricated stamps are hard stamps for thermal imprinting, bendable metal stamps for roll embossing and transparent stamps for UV-imprinting.

Silicon is a material often used for fabrication of hard stamps for thermal imprinting. Fabrication process of silicon stamps was demonstrated using both the imprinted resist and lift-off process for pattern transfer into silicon.

Bendable metal stamp for roll-to-roll application was fabricated using sequential imprinting to fabricate a polymer mold. The polymer mold was used for fabrication of a nickel copy in subsequent electroplating process. Thus fabricated metal stamp was used in a roll-to-roll imprinting process to transfer the patterns onto a CA film successfully.

Polymer stamp for UV-imprinting was fabricated by patterning fluorinated polymer templates using sequential imprinting and a silicon stamp. The imprinted polymer stamp was used succesfully for UV-NIL.

In the stamp fabrication process the features of the silicon stamp were replicated with good fidelity, retaining the original dimensions in all of three stamp types. The results shows, that the sequential imprinting is as a potential stamp replication method for various applications.

ISBN
978-951-38-7726-2 (soft back ed.)
978-951-38-7727-9 (URL: http://www.vtt.fi/publications/index.jsp)

Series title and ISSN	Project number
VTT Publications 1235-0621 (soft back ed.) 1455-0849 (URL: http://www.vtt.fi/publications/index.jsp)	72247

Date	Language	Pages
March 2011	English, Finnish abstr.	70 p. + app. 59 p.

Name of project	Commissioned by

Keywords	Publisher
Nanoimprinting, hot embossing, stamp replication	VTT Technical Research Centre of Finland P.O. Box 1000, FI-02044 VTT, Finland Phone internat. +358 20 722 4520 Fax +358 20 722 4374

Julkaisun sarja, numero ja raporttikoodi

VTT Publications 758
VTT-PUBS-758

Tekijä(t)
Tomi Haatainen

Nimeke

Painomuottien valmistus sekventiaalista nanokuviointimenetelmää käyttäen

Tiivistelmä

Nanoimprint-litografia on noussut varteenotettavaksi ehdokkaaksi nanorakenteiden kuvioinnissa. Tähän asti käytetty optinen litografia on toistaiseksi kyennyt vastaamaan haasteeseen viivanleveyden pienentyessä. Menetelmän kehittäminen johtaa yhä kalliimpiin ja teknisesti mutkikkaampiin ratkaisuihin. Pienempiin viivanleveyksiin on mahdollista käyttää esim. elektronisuihkulitografiaa, mutta menetelmän haittapuolena on massatuotannon esteeksi nouseva hitaus, mikä nostaa kustannuksia.

Nanoimprint-litografian pullonkaulana on ollut painomuottien eli leimasinten valmistus, joka tapahtuu elektronisuihkulitografialla. Pinta-alaltaan suurien muottien valmistus on hidasta ja tulee erittäin kalliiksi. Vaihtoehtoisesti voidaan valmistaa pieni muotti, jota toistamalla voidaan kuvioida laajoja alueita. Tällä menetelmällä voidaan tehdä suuri määrä kopioita alkuperäisestä muotista tai valmistaa suuri kokonaisuus yhdistelemällä erityyppisiä pieniä muotteja.

Tämän väitöskirjatyön aiheena on painomuottien valmistaminen step and stamp nanoimprint-litografiamenetelmällä. Työn kokeellinen osa käsittää prosessiparametrien optimoinnin laajojen alueiden kuviointiin, sekä muottien valmistuksen ja kopioinnin termoplastiseen polymeeriin. Kuviointi tehtiin käyttämällä piistä valmistettua eli leimasinta. Leimasimet valmistettiin pääosin piistä käyttämällä UV- tai elektronisuihkulitografiaa, sekä kuivaetsausta. Menetelmää sovellettiin piipainomuottien kopiointiin, valmistettiin nikkelinen taipuisa painomuotti rullapainomenetelmää varten, sekä läpinäkyvä polymeeripainomuotti UV-imprint-litografiaa varten.

ISBN
978-951-38-7726-2 (nid.)
978-951-38-7727-9 (URL: http://www.vtt.fi/publications/index.jsp)

Avainnimeke ja ISSN	Projektinumero
VTT Publications 1235-0621 (nid.) 1455-0849 (URL: http://www.vtt.fi/publications/index.jsp)	72247

Julkaisuaika	Kieli	Sivuja
Maaliskuu 2011	Englanti, suom. tiiv.	70 s. + liitt. 59 s.

Projektin nimi	Toimeksiantaja(t)

Avainsanat	Julkaisija
Nanoimprinting, hot embossing, stamp replication	VTT PL 1000, 02044 VTT Puh. 020 722 4520 Faksi 020 722 4374

VTT CREATES BUSINESS FROM TECHNOLOGY
Technology and market foresight • Strategic research • Product and service development • IPR and licensing • Assessments, testing, inspection, certification • Technology and innovation management • Technology partnership

VTT PUBLICATIONS

740 Mikko Pihlatie. Stability of Ni-YSZ composites for solid oxide fuel cells during reduction and re-oxidation. 2010. 92 p. + app. 62 p.

741 Laxmana Rao Yetukuri. Bioinformatics approaches for the analysis of lipidomics data. 2010. 75 p. + app. 106 p.

742 Elina Mattila. Design and evaluation of a mobile phone diary for personal health management. 2010. 83 p. + app. 48 p.

743 Jaakko Paasi & Pasi Valkokari (eds.). Elucidating the fuzzy front end – Experiences from the INNORISK project. 2010. 161 p.

744 Marja Vilkman. Structural investigations and processing of electronically and protonically conducting polymers. 2010. 62 p. + app. 27 p.

745 Juuso Olkkonen. Finite difference time domain studies on sub-wavelength aperture structures. 2010. 76 p. + app. 52 p.

746 Jarkko Kuusijärvi. Interactive visualization of quality Variability at run-time. 2010. 111 p.

747 Eija Rintala. Effects of oxygen provision on the physiology of baker's yeast *Saccharomyces cerevisiae*. 2010. 82 p. + app. 93 p.

748 Virve Vidgren. Maltose and maltotriose transport into ale and lager brewer's yeast strains. 2010. 93 p. + app. 65 p.

749 Toni Ahonen, Markku Reunanen & Ville Ojanen (eds.). Customer value driven service business development. Outcomes from the Fleet Asset Management Project. 2010. 43 p. + app. 92 p.

750 Tiina Apilo. A model for corporate renewal. Requirements for innovation management. 2010. 167 p. + app. 16 p.

751 Sakari Stenudd. Using machine learning in the adaptive control of a smart environment. 2010. 75 p.

752 Evanthia Monogioudi. Enzymatic Cross-linking of β-casein and its impact on digestibility and allergenicity. 2010. 85 p. + app. 66 p.

753 Jukka-Tapani Mäkinen. Concurrent engineering approach to plastic optics design. 2010. 99 p. + app. 98 p.

754 Sanni Voutilainen. Fungal thermostable cellobiohydrolases. Characterization and protein engineering studies. 2010. 98 p. + app. 55 p.

756 Tuomas Pensala. Thin Film Bulk Acoustic Wave Devices. Performance Optimization and Modeling. 2011. 97 p. + app. 73 p.

758 Tomi Haatainen. Stamp fabrication by step and stamp nanoimprinting. 2011. 70 p. + app. 59 p.

ISBN 978-951-38-7726-2 (soft back ed.)
ISSN 1235-0621 (soft back ed.)
ISBN 978-951-38-7727-9 (URL: http://www.vtt.fi/publications/index.jsp)
ISSN 1455-0849 (URL: http://www.vtt.fi/publications/index.jsp)